Histol Histopathol (1999) 14: 597-626

http://www.ehu.es/histol-histopathol

Histology and Histopathology

Invited Review

Ribonuclease-gold labels proteoglycan-containing cytoplasmic granules and ribonucleic acid-containing organelles - A survey

A.M. Dvorak and E.S. Morgan

Departments of Pathology, Beth Israel Deaconess Medical Center and Harvard Medical School, Boston, MA, USA

Summary. An enzyme-affinity-gold method to detect RNA in routinely prepared ultrastructural samples is based on the affinity of the gold-coupled enzyme, ribonuclease, for its substrate, RNA. High concentrations of a known inhibitor of RNase, heparin, are uniquely located in human mast cell granules. Specific labeling for the presence of heparin in these structures was determined using the RNase-gold (R-G) reagent based on the RNase inhibitor property of heparin. This property was used to probe for the presence of proteoglycans (PG) known to be present in a wide variety of ultrastructural samples, none of which contain heparin. In addition to known subcellular sites of RNA, the R-G reagent was shown to bind to PG-rich cytoplasmic granules in a wide variety of leukocytes and secretory cells of epithelial, endocrine, and neuroendocrine origin. This newly recognized property was used to image the changing distribution of labeled PGs during cellular maturation, secretion, and recovery from secretion of secretory cells *in vivo*, *ex vivo*, *in vitro* and in isolated, biochemically defined guinea pig basophil granule preparations.

Key words: RNase-gold, Proteoglycans, Secretory granules, Ultrastructure, Mast cells

1. Introduction

Enzyme-affinity-gold ultrastructural cytochemistry was initiated in 1981 when ribonuclease was coupled to colloidal gold particles and used to label intracellular sites of ribonucleic acid (RNA) (Bendayan, 1981). Since then, ribonuclease-gold (R-G) has been used for this purpose in many studies (Bendayan, 1981, 1982, 1984, 1985, 1989; Cheniclet and Carde, 1987; Brooks and Binnington, 1989; Cheniclet and Bendayan, 1990) and the principle extended to the identification of other enzyme substrates by constructing new enzyme-gold probes for this purpose. Among the substrates imaged at high magnification in optimally preserved ultrastructural samples are DNA (Bendayan, 1981, 1982, 1984, 1985, 1989), collagen (Bendayan, 1984, 1985, 1989), elastin (Bendayan, 1984, 1985, 1989), glycogen (Bendayan, 1984, 1985, 1989), hyaluronic acid (Londoño and Bendayan, 1988; Bendayan, 1989), sialic acid (Londoño and Bendayan, 1988; Bendayan, 1989), glucosides (Bendayan and Benhamou, 1987; Bendayan, 1989), histamine (Dvorak et al., 1993, 1994a,b, 1995, 1996b, c, 1997; Dvorak and Morgan, 1996, 1997), mannose (Bendayan, 1989), pectin (Bendayan, 1989), and phospholipid (Bendayan, 1989).

The initial study with R-G used rat pancreatic acinar cells (RPACs) to image RNA (Bendayan, 1981). Precise and specific localization was reported in ribosomes and nucleoli, structures known to contain RNA. One of the necessary specificity controls for enzyme-affinity cytochemistry is to show that binding is diminished or eradicated when inhibitors of the enzyme in question are used (Bendayan, 1981). For ribonuclease, one well-known inhibitor is heparin (Lindahl and Höök, 1978; Mendelsohn and Young, 1978; Chirgwin et al., 1979; Jaques, 1980).

Human mast cell (HMC) granules store proteoglycans which have been shown primarily to consist of heparin (and smaller quantities of chondroitin sulfate E) (Stevens et al., 1988; Thompson et al., 1988), a macromolecule said to be the most anionic substance in the body (Anderson and Wilbur, 1951; Salmivirta et al., 1996) and to be unique to mast cell granules (Lindahl and Höök, 1978; Salmivirta et al., 1996). Historically, the anionic charge of heparin and heparin-protein granule complexes is thought to be the basis for dye binding that facilitates the recognition of mast cells (Uvnäs et al., 1970; Lagunoff, 1974; Wingren and Enerbäck, 1983) as well as to provide "false positives" in imaging techniques based on highly positively charged avidin, in light microscopic preparations (Bussolati and Gugliotta, 1983; Tharp et al., 1985). It is thought that this unique property of heparin serves to

Offprint requests to: Dr. Ann M. Dvorak, M.D., Department of Pathology, East Campus, Beth Israel Deaconess Medical Center, 330 Brookline Avenue, Boston, MA 02215, USA

inhibit RNase in biochemical studies (Lindahl and Höök, 1978; Mendelsohn and Young, 1978; Chirgwin et al., 1979; Jaques, 1980).

We thought that these properties and the known affinity of heparin for ribonuclease might prove useful in imaging heparin, using optimally prepared electron microscopic samples. We selected the human mast cell granule to study first, since it is a unique site of large amounts of heparin and since it should not contain RNA, the substrate for which the R-G method was developed (Dvorak and Morgan, 1998a, 1999). We also examined R-G labeling in guinea pig basophil granules (Dvorak and Morgan, 1998b), since subcellular isolation and biochemical analysis of their single granule population shows that they do not contain heparin but do primarily contain chondroitin sulfate (Orenstein et al., 1978, 1981).

Cytoplasmic granules are membrane-bound organelles which subserve storage, processing, secretory and digestive functions, depending on the cell type within which they reside. Most granules are rendered electron-dense with standard ultrastructural methods; some have variegated patterns, and they vary in size from ~100 nm to several microns in diameter in standard thin sections. While none of the cell types containing these granules contains heparin (with the exception of the mast cell), most of them contain other proteoglycans. We examined a number of cell lineages with cytoplasmic granules (using the R-G method) to determine the potential universality of imaging proteoglycans in their subcellular locations. These studies provide the basis for this review and reveal a wider application of the R-G method - i.e., as an inhibitor which binds to proteoglycans in ultrastructural samples.

2. Ribonuclease-gold method and specificity controls

Electron microscopic samples of tissue and isolated, purified and/or cultured mast cells (human, rat, mouse), basophils (human, guinea pig, rabbit), purified guinea pig basophil granules, eosinophils (human, guinea pig), cloned, granulated mouse lymphocytes, human platelets, guinea pig megakaryocytes, neutrophils (human, mouse, guinea pig, rat), human type II alveolar pneumocytes, human endothelial cells, guinea pig Kurloff cells, rat pancreas acinar cells, glucagon-secreting cells of the human pancreas islet, calcitonin-secreting cells of the human thyroid, neuroendocrine cells of human lung, ileum and stomach, prolactin- and growth hormone-secreting cells of human pituitary, and macrophages (human, guinea pig, mouse) provided the basis for this review.

The samples were fixed routinely in a mixture of aldehydes, either post-fixed in collidine-buffered osmium tetroxide, in potassium ferrocyanide-reduced osmium (or not treated with osmium), stained en bloc in uranyl, dehydrated in a graded series of alcohols and infiltrated in a propylene oxide-Epon sequence and embedded in Epon 812, which was polymerized at 60 °C for 16 hours, all as previously reported (Dvorak, 1987). Thin sections were cut with a diamond knife and were placed on gold or nickel grids and then air-dried before staining.

A colloidal gold suspension (Frens, 1973) was prepared as follows. Four milliliters (4 ml) of a 1% aqueous solution of sodium citrate were added to 100 ml of a boiling aqueous solution of 0.01% tetrachloroauric acid and boiled for 5 minutes. The RNase-gold (R-G) complex was prepared according to the method of Bendayan (1981). Briefly, the colloidal gold suspension was adjusted to pH 9.0 with 0.2M K_2CO_3, and 10 ml of this solution were added to a siliconized tube containing 0.1 to 0.7 mg RNaseA dissolved in 0.1 ml distilled H_2O. The mixture was centrifuged at 25,000 rpm for 30 minutes at 4 °C, using a Beckman 50.2 Ti rotor. The dark red sediment of the reagent (and one of colloidal gold only) were separately resuspended in 3 cc of phosphate-buffered saline (PBS), pH 7.5, containing 0.2 mg/ml of polyethylene glycol.

Grids containing sections were inverted and floated section-side-down on a phosphate-buffered saline (PBS) drop for 5 minutes, followed by incubation on a drop of R-G for 1 hour at 37 °C, pH 7.5. The grids were washed sequentially in PBS and distilled water and stained with lead citrate for 3-10 minutes prior to examination by electron microscopy.

A number of specificity controls were done (Dvorak and Morgan, 1998a,b, 1999). Samples were stained with the uncomplexed colloidal gold suspension alone, with an irrelevant protein-gold complex (bovine serum albumin-[BSA]-gold), with an irrelevant enzyme-gold complex (deoxyribonuclease-[DNase]-gold), or with an inactivated R-G complex that had been heated at 100 °C for 10 minutes. Agar blocks, containing macromolecules (RNA, [16 mg/ml], heparin [20-30 mg/ml], polyuridine [poly U, 10 mg/ml], polyadenine [poly A, 20 mg/ml], chondroitin sulfate (CS) [26 mg/ml], and histamine [53 mg/ml]), were fixed and processed as tissue blocks or cell suspensions and were stained with R-G, or with gold suspension alone. Exposure of the substrate in samples and the R-G reagent to a variety of enzymatic or acidic digestions was done. These included incubations of sections en grid or the R-G reagent with RNase (0.5-1.0 mg/ml), DNase (1 mg/ml), heparinase I (1 mg/ml), histaminase (2.2 mg/ml), proteinase K (0.25 mg/ml), pronase E (0.5 mg/ml), or 0.1N hydrochloric acid (HCl). In some cases, incubations of samples with enzymes together or in sequential order preceded staining with R-G.

Cationized ferritin (CF) (0.5 ml in 10 ml Hanks' balanced salt solution) and cationized colloidal gold (poly-L-lysine [PLL] bound to 10 nm gold) were used to stain cells directly in sections placed on grids. Some samples that were stained with either CF or cationized gold en grid were then stained with R-G. Additional samples were studied in which either the grids carrying them or the enzyme-gold reagent were incubated with

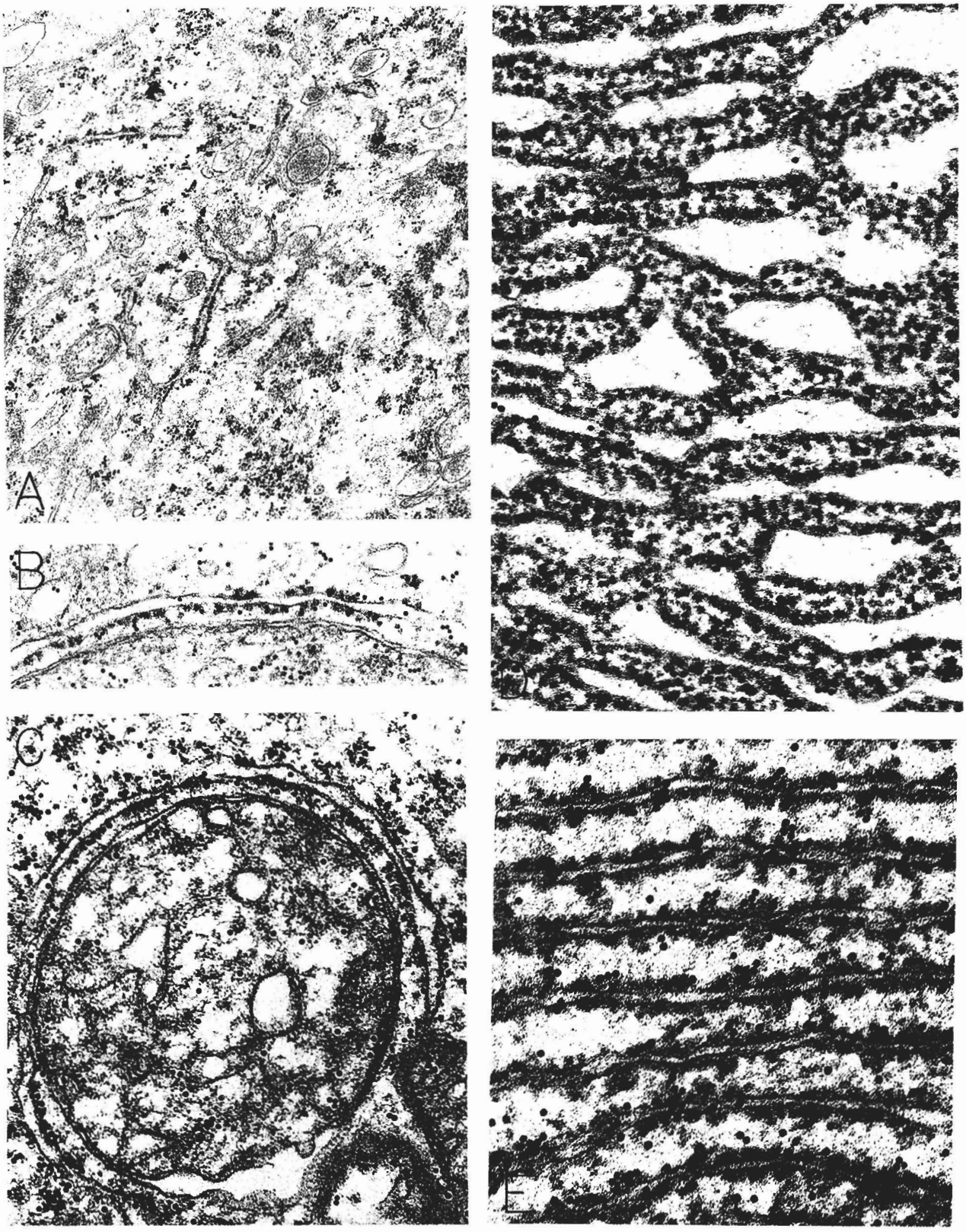

Fig. 1. Examples of ribosome binding of R-G on rough endoplasmic reticulum (RER) of guinea pig megakaryocyte **(A)**, prolactin-secreting cells in a prolactinoma arising in human pituitary **(B, C)**, rat pancreas acinar cell (RPAC) **(D)**, and calcitonin-secreting cells in a metastatic medullary carcinoma arising in human thyroid **(E)**. Note that the cisterns of the RER are generally free of gold label. In (A), clusters of free cytoplasmic ribosomes also bind R-G. The R-G-labeled strands of RER in the prolactinoma cells (B, C) closely surround giant mitochondria. A, x 28,000; B and C, x 54,500; D, x 85,000; E, x 88,500

the following reagents either individually or in various combinations: PLL (0.5 mg/ml), BSA (1 mg/ml), human serum albumin (HSA) (5%), normal goat serum (NGS) (5%), chondroitin sulfate (3 mg/100 μl), DNA Type I (1 mg/ml), gammaglobulin (1 mg/ml), polyvinyl sulfate (0.1 mg/ml), protamine (1 mg/ml), guanidine HCl (1 mg/ml), sodium arsenate (0.001 or 0.002M) histamine (1-2 mg/ml), RNA (1 mg/ml), heparin (1-2 mg/ml). Finally, samples were stained en grid with R-G previously absorbed with heparin-agarose beads or Sepharose beads, with or without additional exposure of the R-G reagent to RNA or heparin, or exposure of the heparin-agarose or Sepharose beads to ribonuclease before adding R-G to the beads.

The results of these specificity controls were quantitated for mast cell granules and expressed as density of gold particles/μm^2 of granule area (Dvorak and Morgan, 1998a).

3. Ribonuclease-gold labels RNA-containing structures in electron microscopic samples

The initial report for the R-G method used this reagent to detect the substrate, RNA, in RPACs (Bendayan, 1981). Precise and specific localization of R-G to nucleoli and ribosomes was demonstrated (Bendayan, 1981). We confirmed these localizations in a wide variety of cell lineages including RPACs (Fig. 1D). Ribosomes exist as free and endoplasmic reticulum-bound particles in the cytoplasm of mammalian cells; in bacteria, RNA-rich areas contain electron-dense ribosomes (Morioka et al., 1986; Kellenberger et al., 1987). R-G specifically bound to ribosomes attached to parallel arrays of rough endoplasmic reticulum (RER) (Fig. 1) in RPACs (Fig. 1D), plasma cells, megakaryocytes (Fig. 1A), calcitonin (C) cells derived from the human thyroid (Fig. 1E), and in prolactin (Fig. 1B,C) and growth hormone secretory cells of the human pituitary. The dilated cisternae of the RER in plasma cells (Fig. 2A) and RPACs (Fig. 1D) did not label for RNA with R-G. Free cytoplasmic ribosomes in all examined cells bound R-G. This was particularly evident in cells without RER as in developing erythroid cells in guinea pig bone marrow (Fig. 2B,C). Also, in bacteria, electron-dense ribosomes avidly bound R-G (Fig. 3).

Nucleoli bound R-G in many cell lineages. Two of these, cultured human type II alveolar epithelial cells and cloned mouse granulated lymphocytes with suppressor activity (Dvorak et al., 1983), showed R-G label overlying portions of giant nucleoli (Fig. 4A,B). Accentuation of label was evident at the periphery of nucleolar dense cords; there was less label in the intervening, less dense nucleolar structures. In nuclei generally, the nuclear matrix bound little label, whereas chromatin-rich areas bound R-G (Figs. 2B, 4A,B). The accentuation of R-G label, as well as labeling with methods to detect DNA, at the edge of nucleolar cords have been noted earlier, and it is postulated that this site is, then, a candidate for the site of nucleolar transcription activity (Ploton et al., 1983; Charest et al., 1985). We also noted that chromosomes extensively bound R-G in granulated lymphocytes with natural killer activity (Galli et al., 1982a; Dvorak et al., 1983) (Fig. 4C), as well as chromosomes found in a number of samples of human tumors with ongoing mitosis. The R-G label uniformly bound to the electron-dense chromatin in these structures. While this pattern of R-G binding could reflect the presence of RNA associated with chromosomes, referred to as chromosomal RNA (Holmes et al., 1972), we cannot rule-out the possibility that some of the extensive nuclear and chromosomal chromatin binding in our samples reflects the presence of nuclear proteoglycans. We have demonstrated the binding of R-G specifically to heparin in human mast cell granules (Dvorak and Morgan, 1998a, 1999) and to chondroitin sulfate in guinea pig basophil granules (Dvorak and Morgan, 1998b), for example (see later). And, numerous methods have shown that nuclei contain sulfated glycosaminoglycans (Bhavanandan and Davidson, 1975; Fromme et al., 1976), in particular chondroitin sulfate (Stein et al., 1975; Hart et al., 1989), heparan sulfate (Hart et al., 1989), hyaluronic acid (Kan, 1990), and heparin (Busch et al., 1992). Functionally, it has been proposed that nuclear proteoglycans may modulate inducible transcription function to promote differentiation in cell development (Busch et al., 1992).

4. Ribonuclease-gold labels heparin in human mast cell granules

Extensive studies of human mast cells (HMCs), isolated from lung or skin and sustained in short-term cultures, developed *de novo* in cultures, or present *in vivo* in multiple sites, formed the basis for our study in which the R-G method was used to identify heparin in HMCs (Fig. 5) in ultrastructural samples (Dvorak and Morgan, 1998a). We performed a large number of controls that were designed to examine the HMC granule binding characteristics of gold alone, of irrelevant protein- or enzyme-gold reagents, of the role of charge and enzyme activity after various enzyme digestions, after blocking with macromolecules, after exposure to inhibitors of RNase and inhibitors of heparin, or exposure to irrelevant enzyme inhibitors. We also stained macromolecule-containing test agar blocks and did a variety of combined absorption and digestion experiments involving the binding of R-G to HMC granules. These studies established that the R-G method detected heparin in HMC granules as well as RNA in conventionally expected sites (Dvorak and Morgan, 1998a). Thus, a new use for this enzyme-affinity-gold technique in mast cell biology was established, based on the known property of heparin as an inhibitor of RNase. The degree of label specificity and ultrastructural detail visibility of the R-G method was equal to or surpassed the existing ultrastructural methods that label mast cell granule heparin (McLaren and Pepper, 1983; Craig et al., 1993; Skutelsky et al., 1995; Oliani et al., 1997).

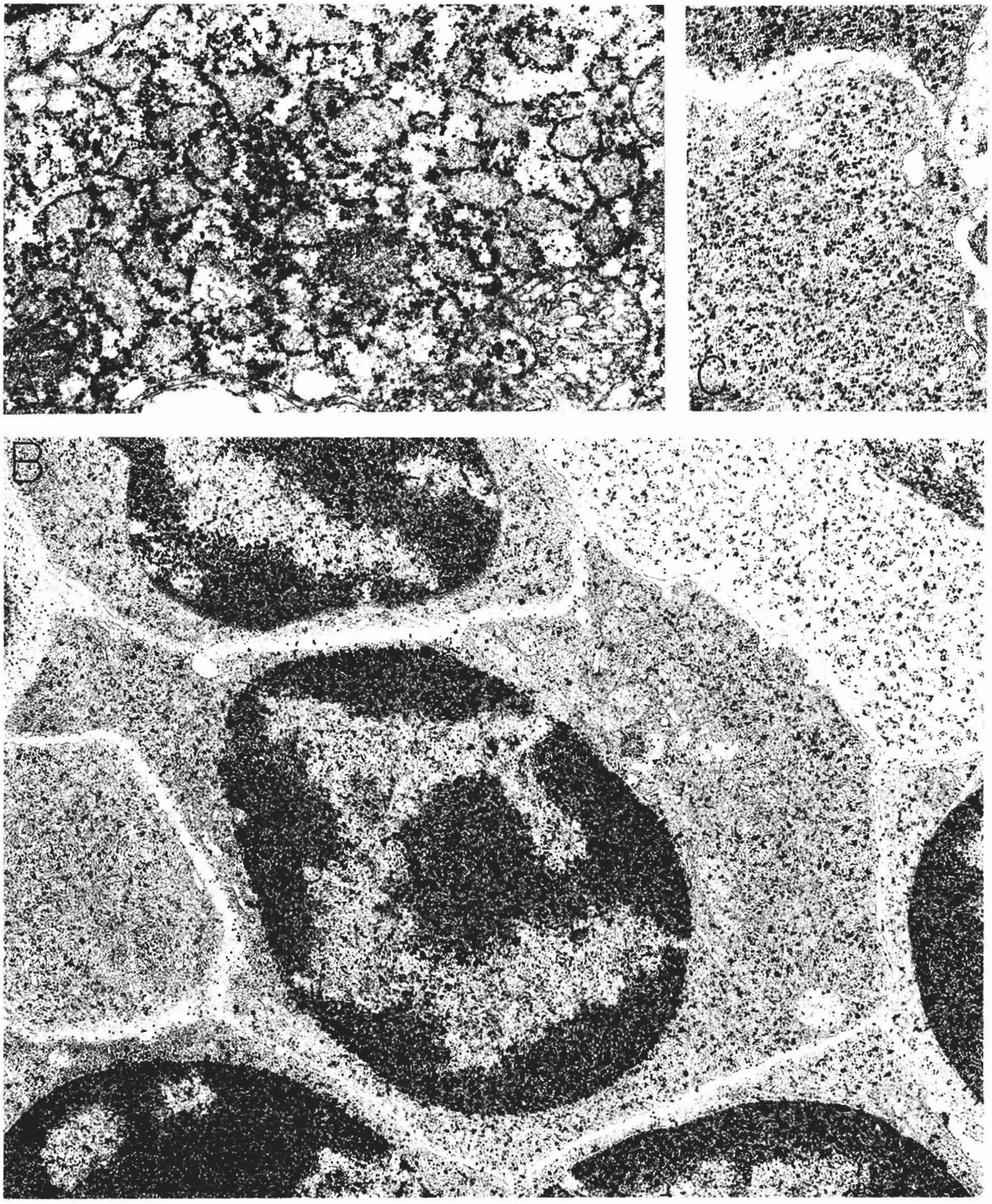

Fig. 2. Membrane-bound and free cytoplasmic ribosome binding in guinea pig plasma cell **(A)** and erythroblasts **(B, C)**. Note that the cisternae of RER in (A) do not bind R-G but that the attached ribosomes do. The cytoplasm of erythroblasts (B, C) have clusters of labeled ribosomes within a homogeneous, organelle-free cytoplasm which contains variable amounts of hemoglobin (gray in panels B and C). These cells, which no longer demonstrate nucleoli, have bound R-G extensively to the condensed chromatin. The nuclei of these cells will be extruded to form anucleate reticulocytes in their next developmental stage (Dvorak et al., 1972). A, x 25,500; B, x 19,500; C, x 30,500

Quantitation of the density of HMC mature granule label for heparin with the R-G method revealed an average of 452.5 gold particles/μm^2 in 15 experiments, to be contrasted with a mean granule density of gold particles of 2.02/μm^2 in 6 experiments of HMCs stained with gold alone.

The specificity of R-G binding for heparin in HMC granules was supported by extensive controls and quantitation (Dvorak and Morgan, 1998a). These controls demonstrated that HMC granules were not labeled with gold alone, with an irrelevant protein-gold conjugate (BSA-gold) or with an irrelevant enzyme-gold complex (DNase-gold). An active enzyme was necessary for a positive binding reaction to HMC granules, as indicated by physical parameters which facilitated granule staining, suggesting that the binding to granules did not rely on charge alone. Charge was further investigated by directly visualizing the prior binding of two cationic electron-dense probes (CF, cationic gold) to HMC granules that blocked subsequent R-G staining. The cationic macromolecule, PLL (used to render the gold cationic), alone also blocked R-G granule staining, implicating charge in the binding reaction.

A series of enzyme or acidic digestions of samples en grid or of the R-G reagent were done. These showed specificity for heparin, since digestion of the sample with heparinase (an enzyme specific for heparin [Linker and Hovingh, 1972]) removed subsequent R-G staining of HMC granules, whereas digestion with histaminase, proteinase, pronase E and DNase did not. Digestions with RNase were technically difficult and resulted in diverse findings, but when proteins were first removed from granules by proteinase or pronase E digestions, followed by RNase digestion, the residual granule heparin stained with increased intensity. Hydrolysis of the sample with HCl did not remove R-G-stainable material from HMC granules. On balance, these studies supported the ability of R-G to stain HMC granule heparin.

A series of macromolecules was used to block R-G staining of HMC granules. Reduction of granule label with R-G was present with heparin or polyvinyl sulfate blocking, both known to be polyanionic competitive inhibitors of RNase (Mendelsohn and Young, 1978; Chirgwin et al., 1979); CS caused a reduction in staining that did not achieve statistical significance. This trend is consistent with biochemical data documenting that the primary proteoglycan in isolated human lung mast cells is heparin, but that a smaller amount of CS is also present (Stevens et al., 1988; Thompson et al., 1988). When heparinase was added to the heparin which was used to block the R-G reagent prior to staining, HMC granule staining was equal to control stains, thus demonstrating that specific inactivation of heparin abrogated the heparin blocking of granule label with R-G. Neither DNA (Fig. 5) nor gammaglobulin blocked R-G binding to HMC granules; RNA caused reductions that did not achieve statistical significance.

Several inhibitors of RNase or heparin were examined. These showed that protamine (a heparin inhibitor that binds to heparin [Linker and Hovingh, 1972; Uvnäs and Åborg, 1976; Jaques, 1980; Rossmann et al., 1982; Taylor and Folkman, 1982]) eradicated R-G binding to HMC granules, as did guanidine HCl (an inhibitor known to solubilize proteoglycans [Lindahl and Höök, 1978; Hay, 1981; Vogel and Peterson, 1981; Rapraeger and Bernfield, 1983; Carlson and Wight, 1987; Thompson et al., 1988; Schick and Eras, 1995]). Incubation of the R-G reagent with sodium arsenate (a DNase inhibitor [Taper, 1979; Bendayan, 1984]) did not reduce subsequent HMC granule binding, thus illustrating that an irrelevant enzyme inhibitor does not interfere with binding of the R-G reagent to heparin.

Histamine, a cation and a major component of HMC granules (Riley and West, 1953; Lagunoff et al., 1961; Login et al., 1992; Dvorak et al., 1993), is bound to granule heparin (Sanyal and West, 1956; Kobayashi, 1962; Lagunoff, 1974; Jaques, 1980), the most anionic substance present in mammalian cells (Anderson and Wilbur, 1951; Salmivirta et al., 1996). We found that exposure of R-G to histamine successfully competed for granule binding with statistically significant reduction in gold label - a finding that was not true when the sample was first incubated in histamine. While heparinase treatment of the sample removed R-G granule staining, treatment with histaminase did not. Previously, we reported that another enzyme-affinity-gold technique, based on the specificity of histaminase (diamine oxidase) for its substrate, histamine, specifically labels histamine in HMC granules and that prior digestion with histaminase removes the diamine oxidase-gold staining from them (Dvorak et al., 1993).

Fig. 3. Bacteria stained with R-G have heavily labeled ribosomes. x 41,000

Test blocks were prepared in agar and processed identically to the electron microscopic samples (Dvorak et al., 1993). Blocks were thin-sectioned and subsequently stained with R-G. Blocks containing heparin or RNA bound R-G. Therefore, the R-G reagent, which we prepare fresh for each staining series, binds to heparin (as in HMC granules) and to RNA (as previously reported [Bendayan, 1981]).

We sought to determine whether the R-G method was detecting RNA in HMC granules as well as heparin. Some of the earliest subcellular fractionation studies of pancreatic zymogen granules reported small amounts of RNA in purified fractions (Meldolesi et al., 1971). The RNA so-detected was considered a contaminant (Meldolesi et al., 1971), an interpretation which is supported by the extremely close alignment of RER with cytoplasmic granules in pancreatic acinar cells and the presence of some RER in granule fractions (Meldolesi et al., 1971). Purified preparations of HMC granules have not been reported. Therefore, similar biochemical composition studies of HMC granules are not available. Since an R-G-stainable component in HMC granules (attributable to RNA) is unexpected, we used a mixture of methods based on enzyme digestions, single, sequential and combined macromolecular blocking with solid substrates to further evaluate this possibility. Prior to adding solid heparin-agarose to these experiments, we determined that RNA blocking in solution did not significantly reduce granule label, whereas heparin and RNA together blocked it, but quantitatively only to the same extent that heparin alone did. When we added the solid substrate heparin agarose, we were able reliably and significantly to block HMC granule staining compared to passage of the R-G reagent over Sepharose beads alone as a control. Altogether, these extensive controls validated use of the enzyme inhibition property of heparin for RNase to image heparin in ultrastructural samples (Dvorak and Morgan, 1998a).

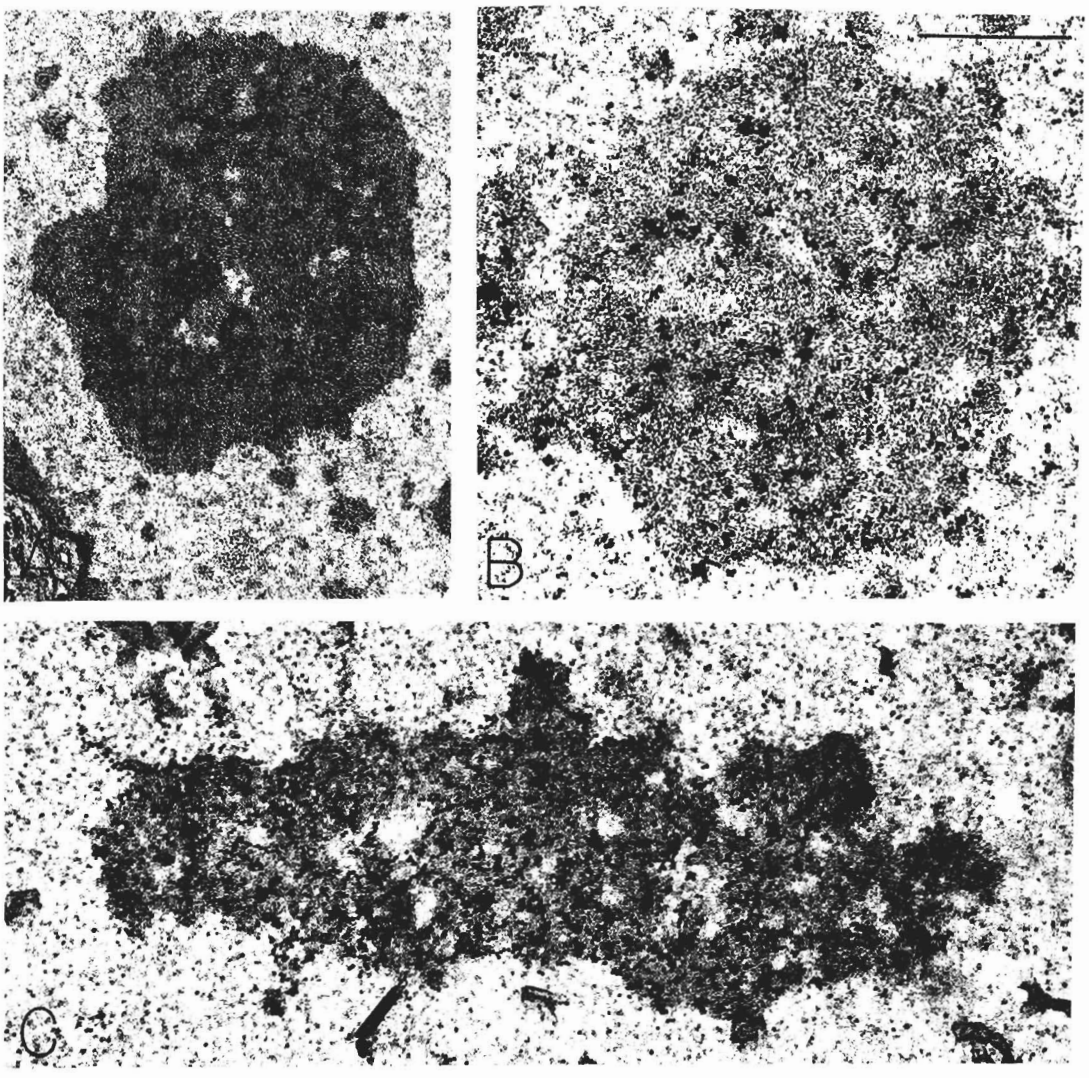

Fig. 4. R-G bound to nucleoli **(A, B)** and a chromosome **(C)** in mouse granulated lymphocytes (A, C) and a human type II alveolar pneumocyte (B). Most of the gold label is associated with the periphery of the dense nucleolar cords in panels A and B. A, x 17,500; B, bar= 0.6 μm; C, x 40,500

5. Distribution of heparin in subcellular sites of human lung mast cells after stimulation and during recovery from secretion

The subcellular locations of heparin in secretory HMCs and HMCs recovering from secretion are not known. As an example of the efficacy of the enzyme inhibitor affinity labeling of heparin, we used the R-G method to image these sites in HMCs which were stimulated to secrete with anti-IgE and which were recovered 20 minutes or 6 hours later for electron microscopic examination (Dvorak and Morgan, 1999). We discovered that heparin was labeled by R-G in electron-dense granules within non-secretory human lung mast cells (HLMCs), in electron-dense granules that persisted in secretory HLMCs at the maximum histamine secretion time (20 minutes), and in electron-dense granules within recovering HLMCs. Heparin stores were absent in newly formed, electron-lucent intracytoplasmic degranulation channels in secretory HLMCs. Electron-dense granule matrices in the process of extrusion to the cell exterior still retained heparin at the instant of cellular secretion. Non-granule heparin stores bound R-G in recovering HLMCs. These locations included resolving degranulation channels, as newly emergent granules partitioned and condensed within them, and electron-dense content-containing vesicles and progranules within synthetic mast cells. Ultimately, all known ultrastructural patterns of HLMC granules developed in recovering cells, and each of them contained heparin. Use of the R-G method allowed the following conclusion: Heparin is secreted from HLMCs when these cells are stimulated by anti-IgE; furthermore, heparin is recovered by a combination of conservative and synthetic mechanisms in HLMCs following a secretory event (Dvorak and Morgan, 1999).

6. Ribonuclease-gold labels CS in guinea pig basophil granules

Basophilic leukocytes are metachromatic granule-containing secretory granulocytes which contain a

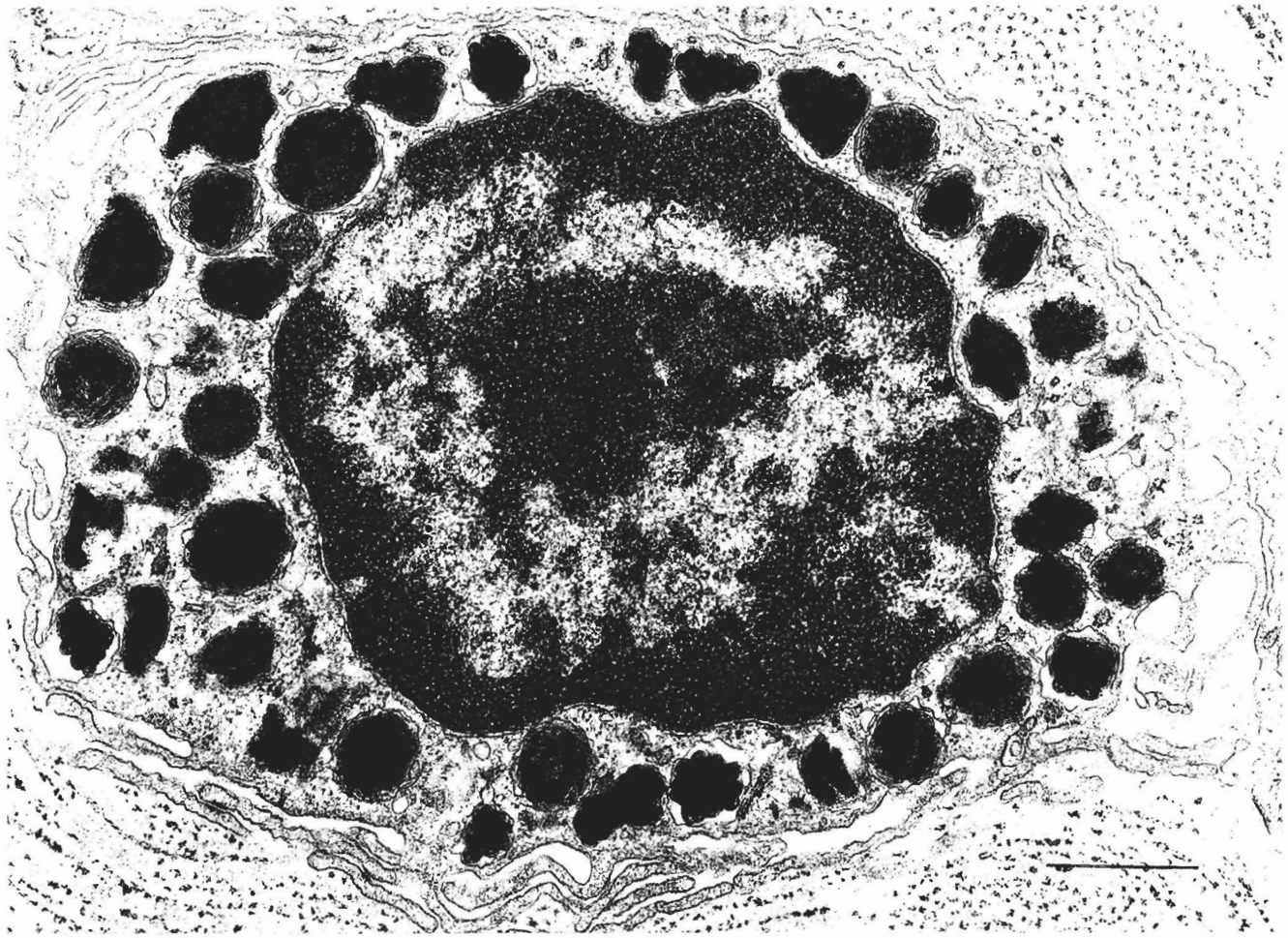

Fig. 5. Human skin mast cell *in vivo* stained with R-G (that was previously incubated with DNA) shows undiminished gold labeling of cytoplasmic granules, nuclear chromatin, and nucleolus. Bar: 0.8 μm.

mixture of granular proteoglycans devoid of heparin. In guinea pigs, isolated granules primarily contain CS (Orenstein et al., 1978, 1981). We used purified guinea pig basophil preparations, cells known to be devoid of heparin (Dvorak et al., 1974), to image other proteoglycans with the R-G method to validate its use for this purpose (Dvorak and Morgan, 1998b). Thus, it is possible that R-G binds to heparin and CS as a competitive inhibitor as well as to RNA by its enzymatic properties. We found that mature granules in guinea pig basophils were labeled with R-G (133 gold particles/μm^2) and that blocking with heparin did not alter the density of granule gold (229/μm^2), but blocking with CS did (0.1/μm^2). Gold alone did not attach to the granules.

Ultrastructural autoradiographic and biochemical analyses of guinea pig basophils have determined that radiolabeled sulfur is incorporated into the granules of these cells (Dvorak, 1978; Orenstein et al., 1978). This indicated that the granules of guinea pig basophils contained sulfur-rich glycosaminoglycans (GAGs), or proteoglycans, which are GAGs linked to a protein core. Orenstein et al. (1978, 1981) characterized the sulfated GAGs in guinea pig basophils and found that most of these macromolecules consisted of a mixture of CS and dermatan sulfate. Smaller amounts were identified as heparan sulfate, but heparin was absent. It was suggested that the highly charged [^{35}S]GAG eluting from DEAE-cellulose with high salt concentrations may represent an oversulfated CS (Orenstein et al., 1978).

In our studies, we used the known proteoglycan composition of guinea pig basophil histamine-rich secretory granules that was determined by biochemical analysis of isolated pure granule fractions (Orenstein et al., 1978) to document that the enzyme-affinity-gold ultrastructural probe, R-G, can specifically bind to CS in basophil granules, which are devoid of heparin. Thus, we confirmed that the R-G method has a wider applicability in electron microscopy - i.e., for imaging of RNA and CS.

7. Distribution of CS in subcellular sites of guinea pig basophils after stimulation and during recovery from secretion

Immature guinea pig basophilic myelocytes developing *in vivo* in the bone marrow are large cells with extensive arrays of cytoplasmic RER and large immature granules which are initially devoid of the crystalline arrays typifying mature granules (Dvorak and Monahan, 1985). When these cells are prepared for electron microscopy with the R-G method, the ribosomes that are attached to the RER bind gold (Fig. 6A). The bound ribosomes and free clusters of polyribosomes are closely adjacent to immature granules. The developing granules bind R-G (Fig. 6A), but to a lesser extent than the mature granules with crystalline substructures (Fig. 6B). As myelocytes mature, the mix of immature granules and RER (Fig. 6A) changes to mature granules and clusters of free ribosomes (Fig. 6B).

We have extensively studied the stimulated degranulation and recovery morphologies of isolated, purified guinea pig basophils (Dvorak, 1978; Dvorak et al., 1981a,b, 1982, 1985, 1987) as well as the morphologies of isolated, purified guinea pig granule preparations (Dvorak et al., 1977). We have prepared similar samples with the R-G method and found that all guinea pig mature granule subtypes - i.e., parallel arrays, hexagonal arrays, finely granular material (Terry et al., 1969; Dvorak, 1978; Dvorak et al., 1981a) - bind R-G. When the basophils are stimulated to undergo anaphylactic degranulation (AND) (Dvorak et al., 1981a), unaltered granules in responding cells retained their crystalline arrays and were labeled with R-G (Fig. 7A). During the course of AND, membrane-free granules are released internally into cytoplasmic degranulation sacs (Fig. 7B) and are extruded to the extracellular space (Fig. 7C). In both instances, the retained parallel arrays of the secreted granules bind small numbers of gold particles (Fig. 7B,C). Isolated granules prepared with their membranes showed that basophil granules labeled extensively with R-G (Fig. 7D); contaminating eosinophil granules in the same preparations were labeled less extensively, and label was absent from their typical central crystals (Fig. 7D). Isolated granules prepared devoid of membranes showed a degree of gold bound to basophil granules (Fig. 7E) that was similar to that for extruded granules from stimulated cells (Fig. 7B,C).

Guinea pig basophils recovering from degranulation were followed in short-term cultures (Dvorak et al., 1982). These mature cells, after being depleted of their granules, developed focal collections of RER and free polyribosomes that were labeled with R-G. Immature granules that developed in these cells progressively became filled with mixtures of vesicles and electron-dense matrix (Dvorak et al., 1982). These materials bound R-G (Fig. 7F,G), a process recapitulating *in vivo* granule maturation in basophilic myelocytes. As increased electron-dense granule matrix condensed in these granules, more R-G was bound to the matrix (Fig. 7F,G).

These findings regarding R-G imaging in developing, secreting and recovering guinea pig basophils show binding to changing locations of RNA-rich free and membrane-bound ribosomes. The changing quantities of granule-bound R-G suggest that CS (Orenstein et al., 1978, 1981; Dvorak and Morgan, 1998b) is progressively added to granules as they mature *in vivo* and *in vitro* and that this proteoglycan is rapidly released from mature crystalline granules that are extruded intra- and extra-cellularly by a degranulating secretogogue, as well as from isolated granule preparations from which granule membranes are removed.

8. Ribonuclease-gold labels CS in human basophil granules

Human basophils are rare granulocytes that are produced in the bone marrow, circulate in mature granulated forms and leave the blood to enter tissues in disease (Dvorak, 1988). They are classic secretory cells

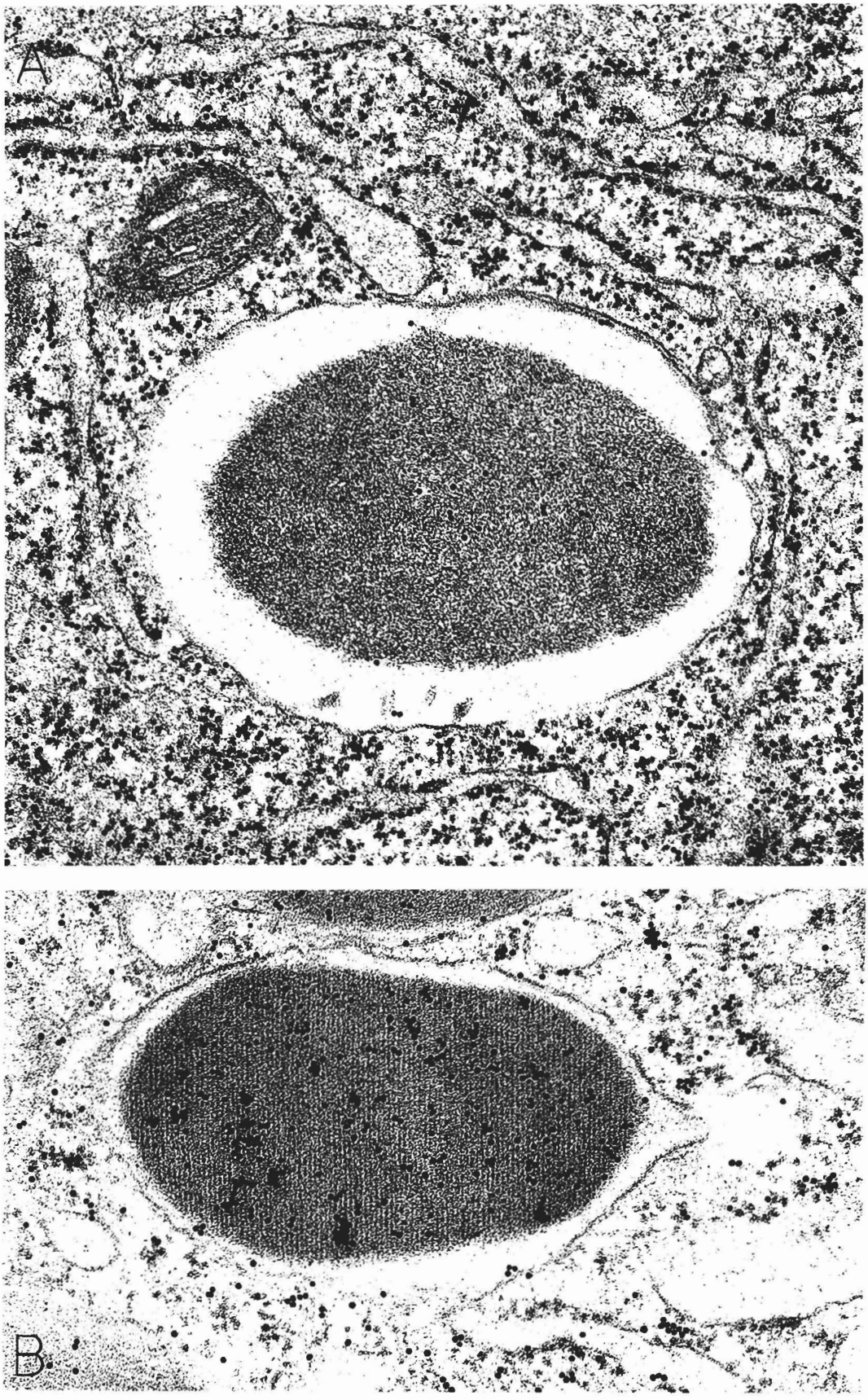

Fig. 6. Guinea pig bone marrow basophilic myelocytes, stained with R-G, show extensive labeling of ribosomes bound to RER (cisternae of the RER do not bind RG) **(A)** and to free clusters of polyribosomes **(B)**. The labeled RER encircles an immature granule in (A) which has moderate R-G staining of the granule matrix. The granule in (B) is a smaller, mature granule displaying a typical parallel array. This granule is extensively labeled with gold particles. A, x 61,000; B, x 69,000

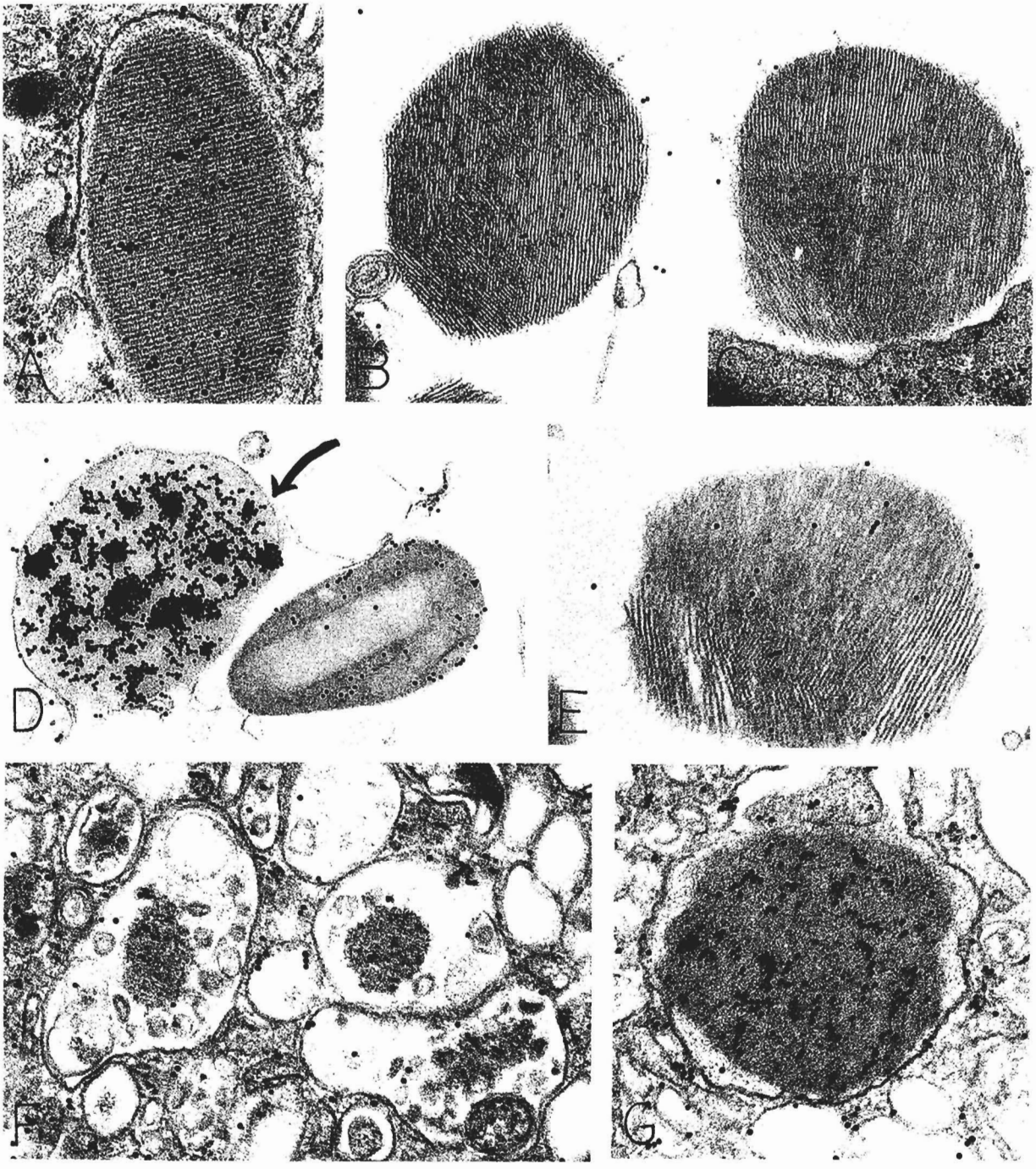

Fig. 7. Guinea pig peripheral blood basophil granules, prepared with R-G. In **(A)**, the parallel array of an unaltered mature granule remaining in a cell that was stimulated to degranulate retains R-G label; in **(B)**, a membrane-free granule, released into a cytoplasmic degranulation sac in a stimulated cell, is labeled minimally; in **(C)**, another membrane-free granule that has been extruded to the extracellular space from a stimulated cell is also labeled minimally. The granules in panels D and E were obtained from purified granule preparations (Dvorak et al., 1977) from partially purified basophils (Dvorak et al., 1974). These preparations were prepared in two ways: (i) to preserve granule membranes **(D)** or (ii) to remove granule membranes **(E)**. Note that the isolated basophil granules retaining their membranes are heavily labeled (arrow, D); the eosinophil mature granule adjacent to it has less label, and the label is confined entirely to the matrix compartment. The central crystal is negative. In (E), the preparation of basophil granules, devoid of membranes, reveals a marked reduction in label similar to the extruded granules from stimulated cells in panels B and C. In **(F, G)**, developing immature granules in basophils that were recovered from an 18-hour culture after a degranulation event are shown. In **(F)**, the membrane-bound immature granules have R-G label over the central electron-dense material. The label is also associated with small peripheral vesicles in the outer granule space. In **(G)**, the condensed, electron-dense granule matrix of a more mature granule binds R-G extensively. A, x 64,000; B, x 46,500; C, x 45,500; D, x 44,500; E, x 56,000; F, x 67,500; G, x 70,000

which also release potent biochemical mediators of inflammation by non-classical, stimulated secretory routes, making use of vesicular transport (Dvorak, 1998). Basophils that have migrated to tissues (in a wide variety of diseases and experimental circumstances) may secrete granule materials into the extracellular milieu. They are effector cells in cutaneous basophil hypersensitivity, a specialized form of cell-mediated hypersensitivity (Dvorak, 1992; Dvorak and Dvorak, 1993). The large cytoplasmic secretory granules in human basophils (Fig. 8A,B) are metachromatic in light microscopic preparations, a property related to the presence of proteoglycans (glycosaminoglycans linked to a protein core) within them (Dvorak, 1988). Ultrastructural autoradiographic studies determined that radiolabeled sulfur was incorporated into human basophil granules (Galli et al., 1984). This indicated that the granule contents of basophils were sulfur-containing proteoglycans.

Biochemical studies of human basophils showed that they contain primarily CS in their secretory granules (Galli et al., 1979; Metcalfe et al., 1984; Ishizaka et al., 1985). These studies were done using basophils from patients with myelogenous leukemia (Galli et al., 1979; Metcalfe et al., 1984) and basophils which developed in human cord blood cell cultures (Ishizaka et al., 1985). Heparin was absent from human basophils (Metcalfe et al., 1984).

Using the RNase-gold ultrastructural method, we found that the CS-rich granules in human basophils could be imaged in electron microscopic samples (Fig. 8A,B). Generally, the electron-dense, particle-packed granules, which are the main morphologic granule type in human basophils (Dvorak, 1988), bound the R-G reagent (Fig. 8A), whereas the small, infrequent para-nuclear granule (described by Hastie [1974]) did not. Finely granular, homogeneously dense material present in some human basophil granules bound R-G (Fig. 8B), whereas Charcot-Leyden crystals embedded within particle-packed granules were conspicuously devoid of R-G label indicating proteoglycans (Fig. 8A). In conjunction with biochemical (Galli et al., 1979; Metcalfe et al., 1984; Ishizaka et al., 1985) and earlier cytochemical analyses (Parmley et al., 1979), designed to demonstrate sulfated glycoconjugates (Spicer, 1965), the new findings obtained with R-G support and extend the localization of CS to human basophil granules.

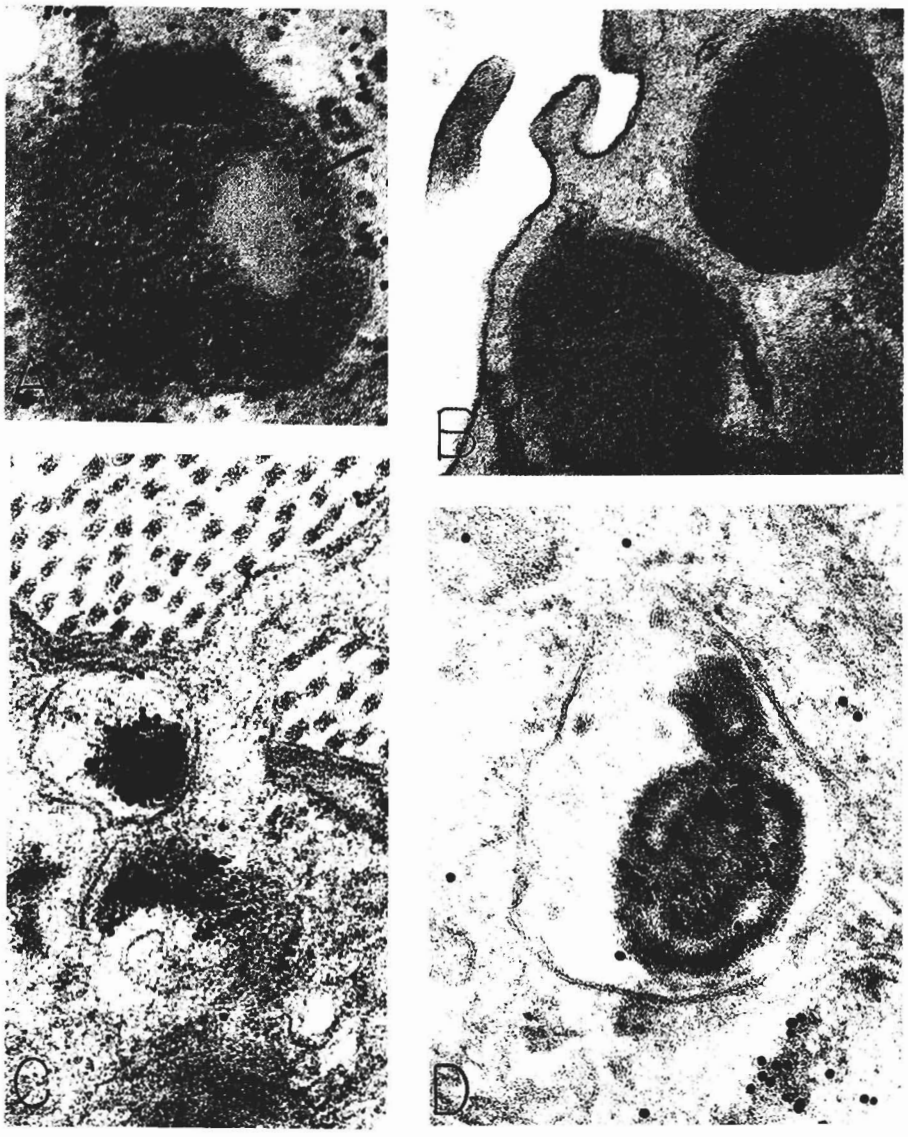

Fig. 8. Human peripheral blood (A,B) and rabbit corneal (C,D) basophils prepared with R-G demonstrate gold-labeled electron-dense structures. In **(A)**, the typical large particulate material of the secretory granule is heavily labeled; the homogeneous Charcot-Leyden crystal (arrow) is not labeled. In **(B)**, less frequently found, homogeneously dense human basophil granules also bind R-G. Rabbit basophil granule electron-dense material, close to the extracellular corneal collagen but still within the cell, binds R-G extensively **(C)**; and, at higher magnification, electron-dense, concentric, thick threads in granules bind R-G. A, x 77,000; B, x 61,000; C, x 69,500; D, x 90,000.

9. Ribonuclease-gold labels proteoglycans in rabbit basophil granules

Rabbit basophils also leave the blood vascular space to enter tissues, such as the rabbit cornea, during inflammation (reviewed in Dvorak, 1992). Rabbit basophil secretory granules have sulfated glycoconjugates, as demonstrated by cytochemistry (Hardin and Spicer, 1971). Their contents are ultrastructurally heterogeneous, displaying mixtures of electron-dense particles, concentric and tangled thick threads, and finely granular materials (Horn and Spicer, 1964; Wetzel et al., 1967; Hardin and Spicer, 1971; Dvorak, 1992). These electron-dense components of rabbit basophils were labeled with the R-G method, indicating the presence of proteoglycans within them (Fig. 8C,D).

10. Piecemeal degranulation of human mast cells in chronic inflammation *in vivo* is accompanied by the secretion of heparin

Human mast cells *in vivo* in chronic inflammatory diseases often show evidence of secretion of their granule contents by a process termed piecemeal degranulation (PMD) (Dvorak et al., 1992; Dvorak and Monahan-Earley, 1995c; Dvorak and Morgan, 1997) (and reviewed in Dvorak, 1992). This process is recognized in mast cells in ultrastructural samples where mast cell granules show variable-to-complete secretion of their granule matrix but retain their membrane-bound containers in the cytoplasm (Fig. 9A,C,E). Often, the same samples show full granules in the same cells. Previously, we have shown that this morphology is associated with histamine secretion *in vivo* (Dvorak and Morgan, 1997) using an ultrastructural enzyme-affinity-gold technique to image histamine (Dvorak et al., 1993). Using the R-G method, we now report that these same cells in human disease also secrete heparin by PMD (Fig. 9). Heparin secretion, demonstrated by this method, was particularly evident in interstitial pulmonary fibrosis (Fig. 9A,D,E) and in Crohn's disease of the ileum (Fig. 9C), both of which are chronic inflammatory diseases of unknown etiology with increased tissue mast cells (reviewed in Dvorak, 1992). In contrast, gastric mucosal mast cells in a patient with a carcinoid tumor of the stomach showed extensive heparin deposits in cytoplasmic granules (Fig. 9B).

11. Ribonuclease-gold labels heparin in rat peritoneal mast cell granules

It has long been known that rat peritoneal mast cells are a rich source of heparin (Lagunoff, 1974; Uvnäs and Åborg, 1977; Yurt et al., 1977), and immunocytochemical (Oliani et al., 1997) and cytochemical (Skutelsky et al., 1995) approaches have been used to demonstrate the granule stores of heparin in rat peritoneal mast cells. One method used heparinase digestions and a cationic-gold method to demonstrate heparin in rat peritoneal mast cell granules (Skutelsky et al., 1995) and obtained results similar to those that we have obtained using the ultrastructural enzyme-affinity-gold method based on the inhibition of RNase by heparin (Fig. 10).

As with the cationic-gold method (Skutelsky et al., 1995), we noted that immature granules with irregular electron-dense materials were largely devoid of heparin (Fig. 10C). Generally, the large, homogeneously electron-dense, mature secretory granules, which typify rat peritoneal mast cells, were heavily labeled with R-G (Fig. 10). Occasional granules similar in appearance to these mature granules in the same mast cells were nearly devoid of label with R-G (Fig. 10B,C). Focal areas within mature granules that contained homogeneously electron-dense material also failed to bind R-G (Fig. 10D). These findings suggest some variability in heparin content in what appear to be (by routine ultrastructural morphology) unaltered, mature granules and foci within mature granules. Immature, condensing granules apparently contain less heparin than is present in mature, fully condensed granules.

12. Ribonuclease-gold labels CS in cultured, bone marrow-derived mouse mast cell granules

Granulated cells were developed from mouse bone marrow, liver or spleen cells in factor-containing culture media and were identified by ultrastructural analysis as immature mast cells (Nabel et al., 1981; Galli et al., 1982b). Extensive studies characterized these cells as expressing Fc_{ε} receptors that bind IgE, containing histamine, incorporating $^{35}SO_4$ into CS (but not into heparin), and containing radiolabeled sulfur in their prominent, immature secretory granules by electron microscopic autoradiography (Nabel et al., 1981; Galli et al., 1982b). Stimulation of these immature mouse mast cells led to classic anaphylactic degranulation of their immature granules in conjunction with histamine secretion (Nabel et al., 1981; Dvorak and Galli, 1987).

We stained similar preparations of cultured, bone marrow-derived, immature mouse mast cells with R-G only or with a combined method including R-G and cytochemistry to detect non-specific esterase(s) (Dvorak et al., 1987). The immature mouse mast cells contained a mixture of homogeneously electron-dense mature granules and immature granules that were filled with small vesicles, focal, electron-dense progranular material and variable proportions of homogeneously dense matrix (Fig. 11). A prominent esterase-positive ectoenzyme was associated with the plasma membrane of these immature mast cells (Fig. 11C). The R-G method stained CS in mature and immature granules in these cells which contain no heparin (Fig. 11). Thus, analogous to labeled granules in human and guinea pig basophils, staining in the immature mouse mast cells further substantiates use of this technique to label CS in cell lineages that do not contain heparin.

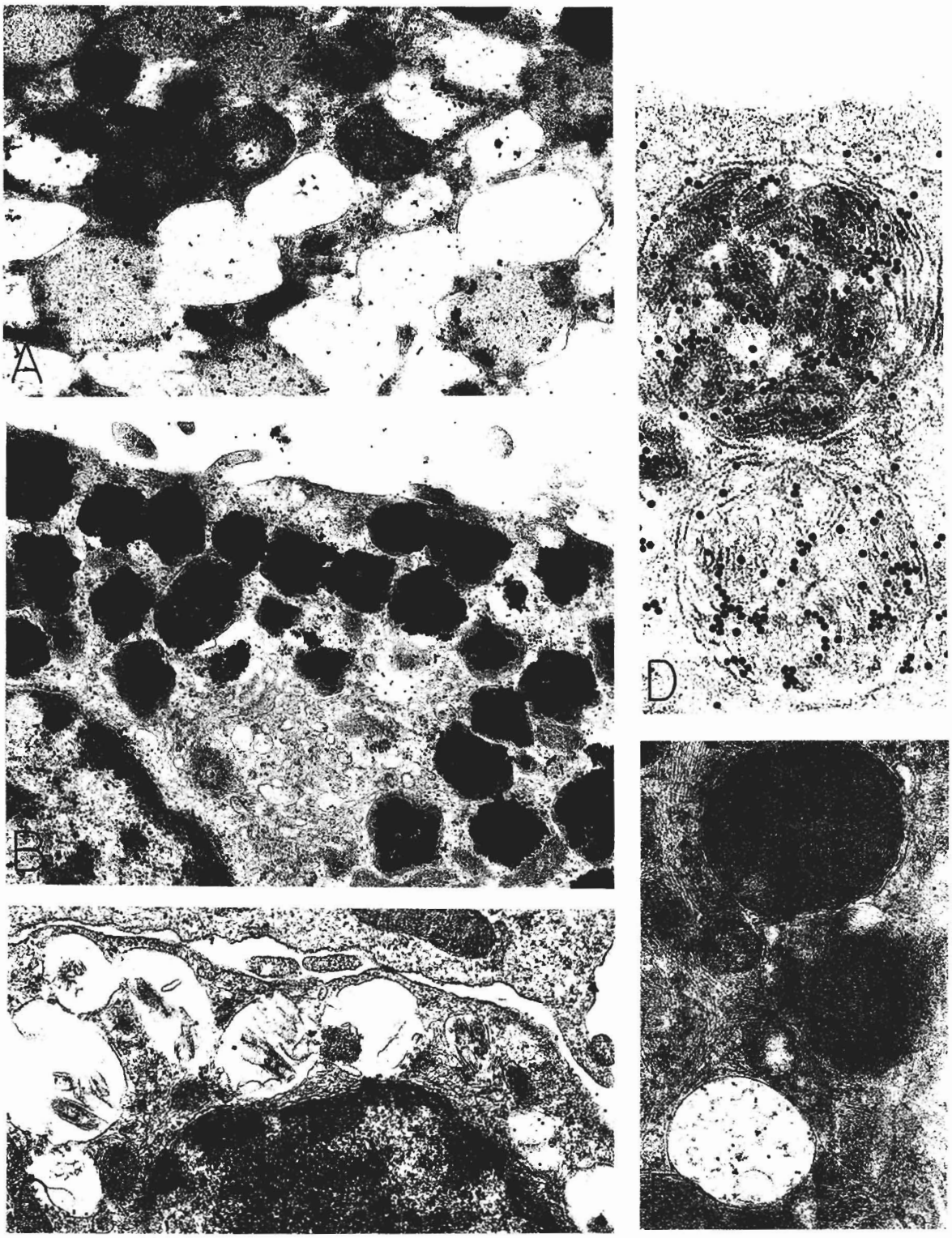

Fig. 9. Human mast cells stained with R-G in lung **(A, D, E)**, gastric **(B)**, and ileal **(C)** specimens obtained from patients with idiopathic pulmonary fibrosis (A, D, E), carcinoid tumor (B), and Crohn's inflammatory bowel disease (C). The mast cells in panels A, C, and E show piecemeal degranulation characterized by residual empty granules from which visible contents have been entirely (A) or partially (A, C, E) secreted. Note residual particles (A, E) and scrolls (C) in some of the partially emptied granules. Granules showing these losses contain little-to-no heparin label (A, C, E), often side-by-side with granules retaining their gold-labeled heparin (A, E). The gastric mucosal mast cell in (B) has extensive heparin label in all secretory granules. The higher magnification views (D, E) show the extent of R-G label in lung mast cell scroll granules with variable packing density of scrolls. A, x 24,500; B, x 25,000; C, x 28,500; D, x 92,000; E, x 33,000

13. Ribonuclease-gold labels proteoglycans in eosinophil, neutrophil, and platelet granules

Numerous reports have characterized proteoglycans in leukocytes and platelets (Olsson and Gardell, 1967; Olsson, 1968; Olsson et al., 1968; MacPherson, 1972; Avila and Convit, 1975; Metcalfe et al., 1982; Levine et al., 1990). In human eosinophils, neutrophils and platelets, the predominant proteoglycan class is CS, whereas heparin is absent. Thrombin-stimulated, washed human platelets secrete proteoglycan and platelet factor 4 (PF4) bound to CS (Levine et al., 1990). A major proteoglycan in platelets is the CS proteoglycan serglycin, which has been shown to have a markedly greater affinity for PF4 than does heparin (Kolset et al., 1996). These reports support the interpretation that the R-G method we used to examine subcellular binding sites in eosinophil (Fig. 12A,B), neutrophil (Fig. 12C,D), platelet (Fig. 12E), and megakaryocyte granules labeled CS in these secretory-storage organelles. In addition to granule label, the R-G method labeled free and membrane-bound ribosomes in the cytoplasm of leukocytes and their progenitors (Figs. 1A, 6). When a classic release reaction was stimulated in human platelets by

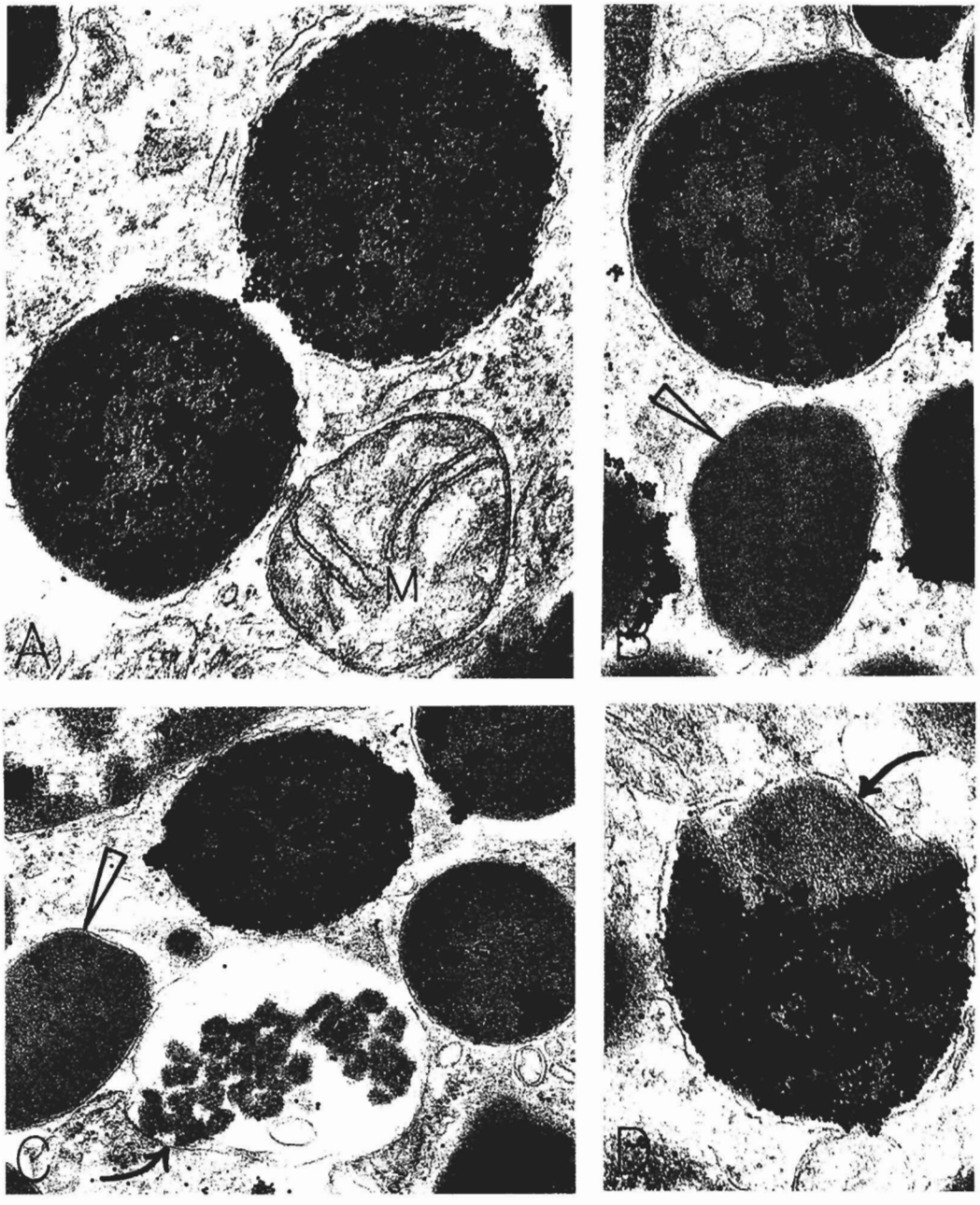

Fig. 10. Rat peritoneal mast cells, prepared with the R-G method, show dense labeling of secretory granule heparin, with little-to-no labeling overlying mitochondria ("M") and adjacent cytoplasm **(A-D)**. Some granules with finely granular, homogeneously dense contents label poorly (arrowheads in B, C). Focal areas of granules displaying a similar content also bind very little R-G in the same granule, which is heavily labeled (arrow, D). Immature granules containing focal deposits of electron-dense material in an electron-lucent background also stain poorly with R-G (arrow, C). A, x 50,500; B, x 45,500; C, x 36,500; D, x 50,500

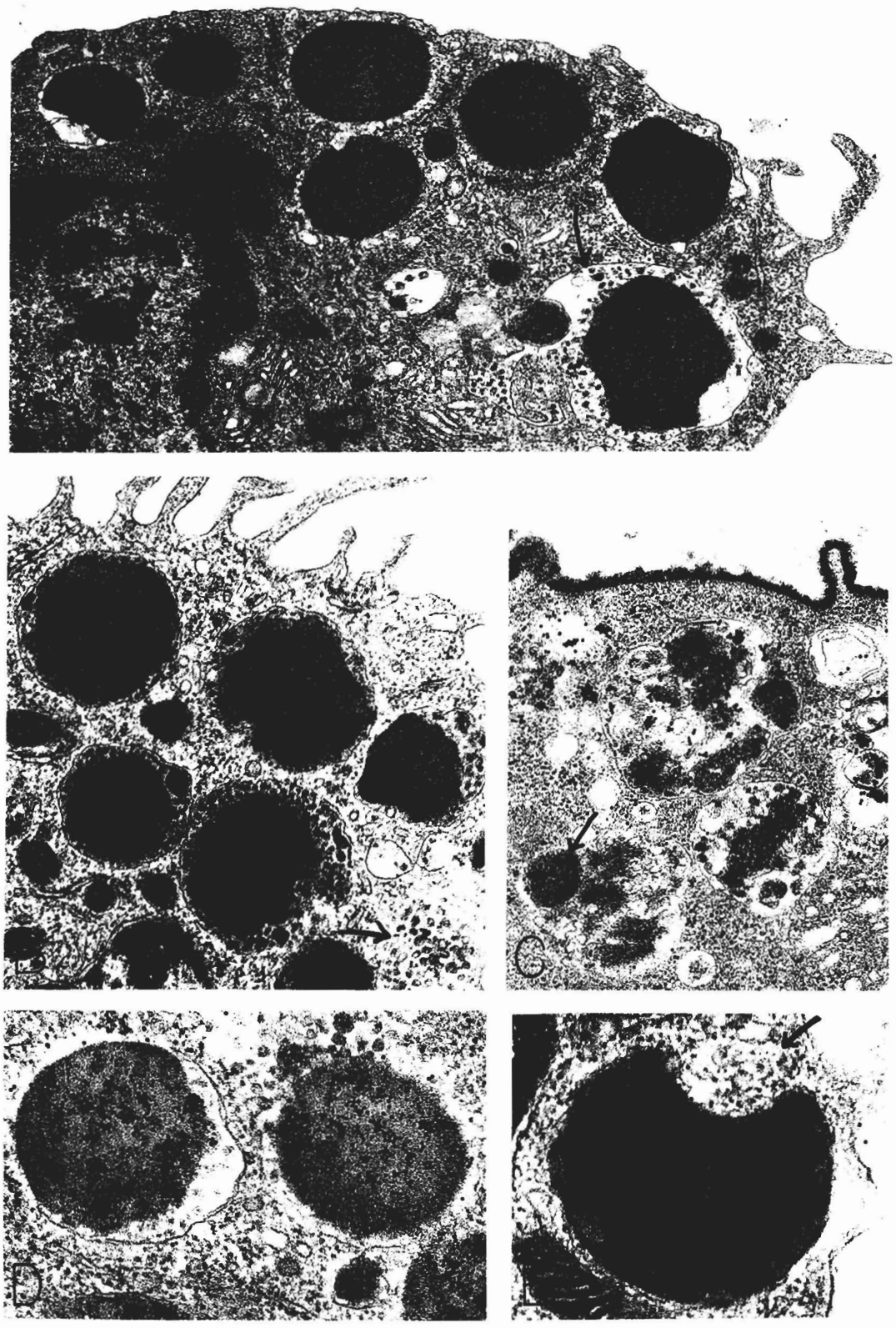

Fig. 11 Immature mouse mast cells cultured from bone marrow (Nabel et al., 1981; Galli et al., 1982b) and prepared with the R-G method **(A-E)** or with a double method, namely R-G and cytochemistry to detect non-specific esterase(s) (C) (Dvorak et al., 1987). A mixture of homogeneously electron-dense mature granules and immature granules with heterogeneous contents (arrow) binds R-G in panel A. Immature granules (B, C) bind R-G predominantly over electron-dense granule material (B) and over progranules (arrow, C) incorporated within the immature granules. The peripherally located vesicular component of immature granules also binds R-G (arrow, B). A prominent esterase ecto-enzyme, bound to the plasma membrane of this immature mouse mast cell, is visible in panel C. Higher magnifications of granules with extensive gold binding are shown in panels D and E. A ribosome-filled portion of cytoplasm that binds R-G has indented a granule (arrow, E). A, x 24,000; B, C, x 33,500; D, x 52,000; E, x 52,500

exposing them to thrombin (Dvorak and Monahan-Earley, 1995i,j), alpha granule contents and fibrin strands within dilated elements of the open canalicular system bound R-G (Fig. 12E).

14. Ribonuclease-gold labels CS in large granulated mouse lymphocytes

Cloned, large granulated mouse lymphocytes with defined function(s), such as natural killer cell or suppressor T lymphocyte functions, are known to contain CS and to incorporate radiolabeled sulfur into their large cytoplasmic granules (Galli et al., 1982a; Dvorak et al., 1983). Additional studies of human lymphocytes (Levitt and Ho, 1983) and rat large granular lymphocyte tumor cells (Stevens et al., 1987) also document the presence of CS in lymphocytes in these two species. When the cloned mouse cells were prepared for electron microscopy with the R-G method, the large, electron-dense cytoplasmic granules bound R-G (Fig. 13A-C). Invaginations of ribosome-containing, gold-labeled fragments of cytoplasm into the cytoplasmic granules - a process analogous to autophagy - was noted (Fig. 13B). Thus, these granules, which are known to

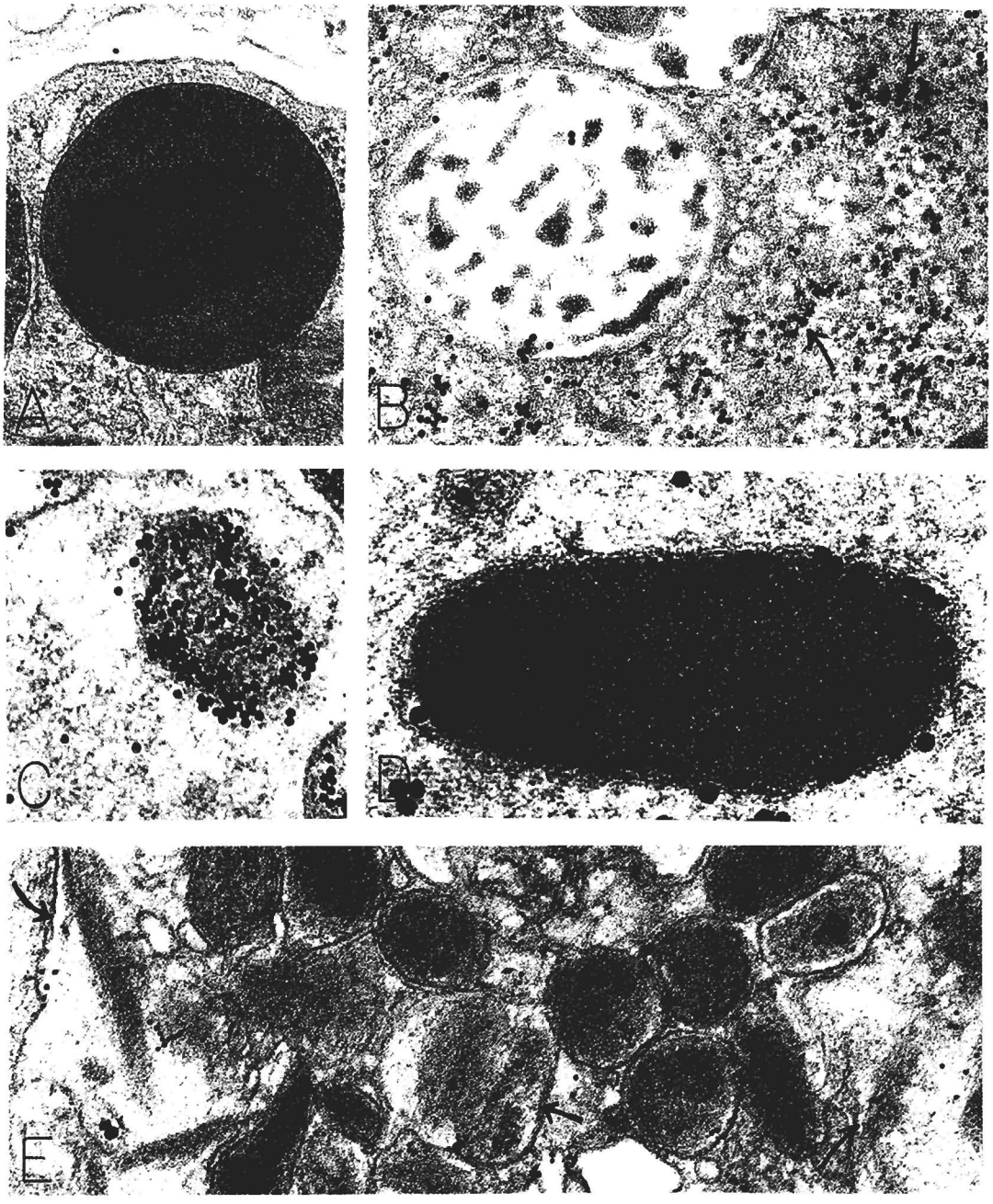

Fig. 12. R-G-stained leukocytes and platelets obtained from guinea pig peripheral blood **(A)**, guinea pig bone marrow **(B, D)**, and human blood **(C, E)**. In (A), a mature eosinophil granule shows R-G label in the matrix compartment which surrounds the central, unlabeled crystalline core compartment. In (B), an immature eosinophil granule in the Golgi region of a guinea pig eosinophilic myelocyte has a few gold particles associated with electron-dense particles which typify immature eosinophil granules in this species. Clusters of cytoplasmic polyribosomes (arrows) nearby are also labeled with R-G. In (C), an azurophilic (primary) granule in a human intravascular neutrophil within a gastric carcinoid tumor is heavily labeled with R-G. In (D), a specific (secondary) granule in a guinea pig neutrophil binds R-G. In (E), this thrombin-stimulated human platelet shows centralized alpha granules labeled with gold and portions of several elements of the open canalicular system (arrows) which contain released alpha granule contents and fibrin strands. These materials also bind R-G. A, x 57,000; B, x 71,500; C, x 81,000; D, x 180,000; E, x 54,000

contain mixtures of secretory and lysosomal products, may acquire R-G-labeled RNA by internalizing cytoplasmic fragments destined for destruction. The binding of R-G to these granules may then represent a mixture of CS and RNA. Granulated mouse lymphocytes also bound R-G to free and membrane-bound ribosomes and to giant-sized nucleoli. The large aggregates of cytoplasmic glycogen, which typify the cloned mouse cells (Dvorak et al., 1983), did not bind R-G.

15. Ribonuclease-gold labels CS-rich Kurloff bodies in guinea pig Kurloff cells

Kurloff cells, unique to guinea pigs, are widely distributed mononuclear cells which contain a large, single, often nucleus-sized granule. These cells are of uncertain lineage and have unknown function(s) (Revell, 1977). The distinctive large cytoplasmic granule is membrane-bound and contains homogeneously electron-dense contents and is referred to as a Kurloff body (Revell, 1977). The material in Kurloff bodies has been isolated and biochemically characterized as CS (Dean and Muir, 1970). These unique structures, which define these cells, were strongly labeled with gold using the R-G method (Fig. 13D). Additionally, smaller, adjacent and attached membrane-bound structures with identical visible contents also bound R-G. In serial electron microscopic sections, others have reported that the smaller structures are all continuous with the large, single, rounded Kurloff body (Revell, 1977). While the function(s) of these unique cells and their Kurloff bodies is not known, the R-G staining supports the biochemical conclusion (Dean and Muir, 1970; Revell, 1977) that much of their contents is CS.

16. Ribonuclease-gold labels secretory granules in rat pancreatic acinar cells (RPACs)

RPACs were the initial cells tested for the detection of RNA, the substrate for which the R-G method was originally developed (Bendayan, 1981). The target organelles, reported to be stained, were nucleoli and ribosomes on the RER (Bendayan, 1981). We here confirm these localizations of R-G binding in RPACs (see Section 3) and describe an additional binding site in

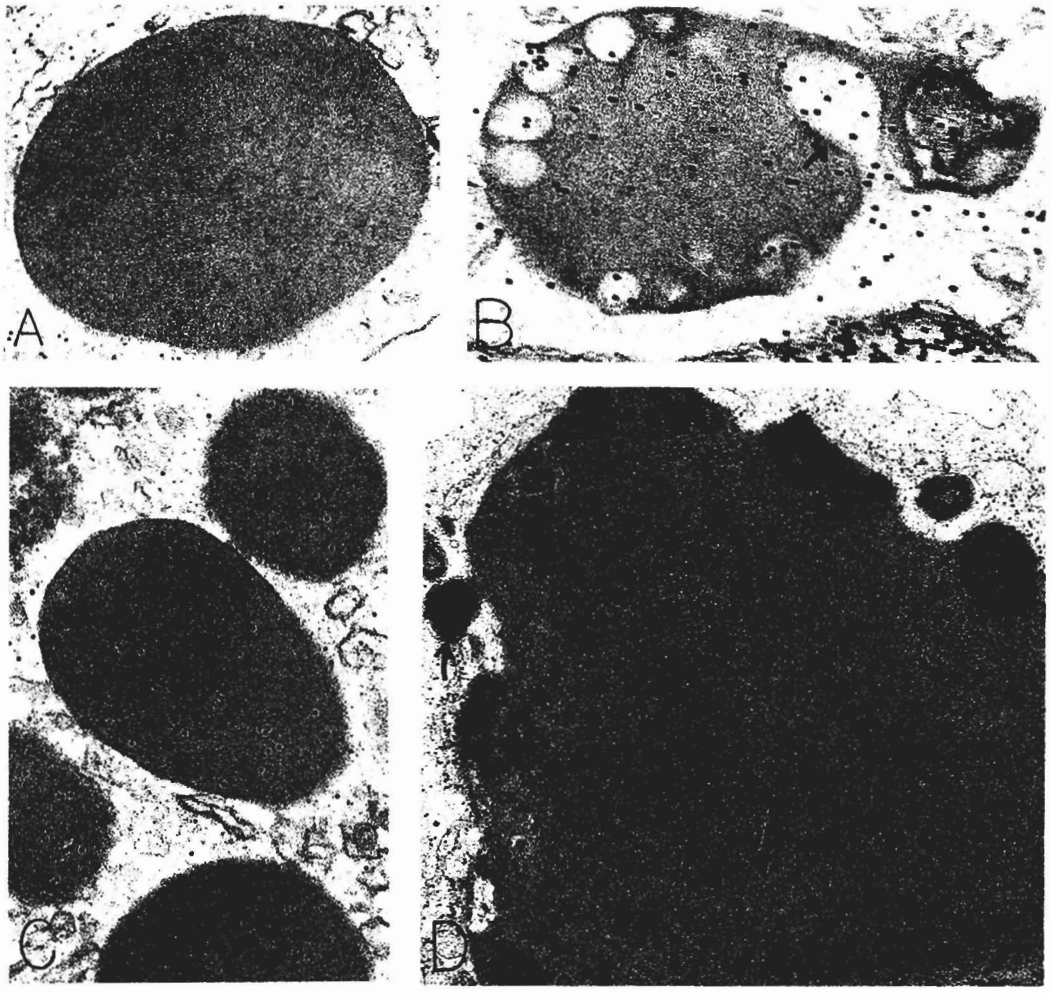

Fig. 13. R-G-stained, large granulated lymphocytes cloned from mice **(A-C)** and a guinea pig Kurloff cell **(D)**. In panels A and B, large, cytoplasmic, membrane-bound granules are gold-labeled with R-G. These cells expressed natural killer (NK) function (Galli et al., 1982a; Dvorak et al., 1983). Note that, in addition to the gold-labeled dense granule matrix, there are multiple invaginations into the granule matrix of ribosome-containing cytoplasm labeled with R-G (arrow). In (C), the labeled, large cytoplasmic granules are in the cytoplasm of a cloned, large, granulated mouse T lymphocyte with suppressor cell function (Dvorak et al., 1983). In (D), a heavily labeled Kurloff body fills the cytoplasm of a guinea pig bone marrow Kurloff cell. A, x 38,500; B, x 51,500; C, x 41,000; D, x 23,500

these exocrine secretory cells - cytoplasmic zymogen granules (Fig. 14). Colloidal gold alone does not bind to these granules. This finding is dissimilar to that in the original report (Bendayan, 1981).

Pancreatic acinar cells are exocrine secretory cells filled with large secretory granules, extensive arrays of RER and active Golgi structures; thus, they are amply endowed with necessary organelles for the synthesis, storage and secretion of their protein products. Their zymogen granules are also known to contain proteoglycans (Kronquist et al., 1977; Reggio and Dagorn, 1978; Reggio and Palade, 1978). Ultrastructural autoradiography of radiolabeled sulfur showed the incorporation of label in guinea pig pancreas acinar cells to be over Golgi structures, condensing vacuoles and zymogen granules (Reggio and Palade, 1978). Biochemical and ultrastructural autoradiographic studies of isolated, purified granules from these cells showed them to contain the radiolabeled sulfur (Reggio and Palade, 1978). The sulfated macromolecular material in pancreatic acinar cell granules is composed principally of CS and heparan sulfate (Kronquist et al., 1977; Reggio and Dagorn, 1978; Reggio and Palade, 1978), not heparin. Early reports that pancreatic acinar cell granules contained up to 1% RNA, the substrate for R-G, were thought to represent minor contaminants of ribosomes in the granule preparations (Greene et al., 1963). Given the often intimate association of free ribosomes and RER with RPAC granules (Fig. 14) and the presence of ribosomes in purified preparations examined by electron microscopy (Greene et al., 1963), this would seem to be a realistic interpretation. Thus, RPAC granules are devoid of RNA, the substrate for R-G (Bendayan, 1981), and heparin, which labels with R-G as an inhibitor of ribonuclease (Dvorak and Morgan, 1998a), making the interpretation that R-G is binding to other proteoglycans in these granules presently the best interpretation.

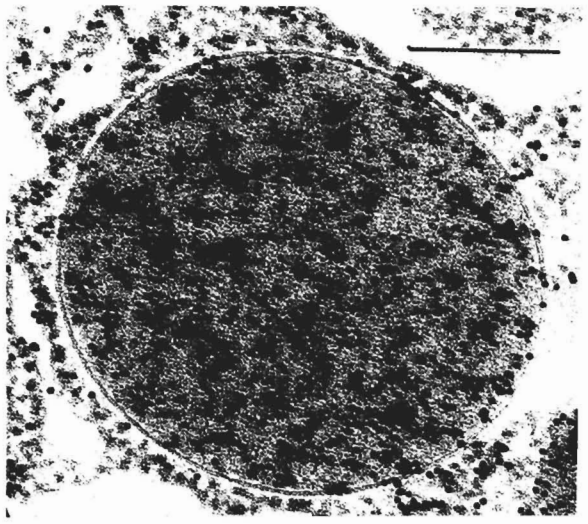

Fig. 14. RPAC granule prepared with the R-G method shows extensive binding of gold to the granule matrix, to the overlying granule membrane, and to free and membrane-bound ribosomes immediately adjacent to the granule. Bar: 0.2 μm.

17. Ribonuclease-gold labels secretory granules in human cells of diverse origins

Since RPACs, classical exocrine secretory cells, bound R-G, probably to proteoglycans within them, we did a survey of a number of human secretory cells of diverse origin(s), including endocrine cells, neuroendocrine cells, lung alveolar cells, and endothelial cells, to substantiate further the ability of R-G to bind to proteoglycans either known or presumed to form an integral part of these granules. In many cases, the samples studied were obtained from patients manifesting clinical expressions of functional syndromes associated with secretion of their unique granule protein products. In virtually all of the samples that we prepared with the R-G method, the specific secretory granules bound R-G (Figs. 15,16). For example, the phospholipid-rich lamellar body, which stores surfactant in type II alveolar pneumocytes (Dvorak and Monahan-Earley, 1992d-f, 1995e,g), binds R-G (Fig. 15A). Weibel-Palade bodies are elongated secretory granules unique to endothelial cells that are known to store the clotting factor, von Willebrand factor (Weibel and Palade, 1964; Dvorak, 1996). They bound R-G in many of the samples that we examined (Fig. 15B). Pancreatic islet cell alpha granules are recognizable by their eccentric electron-dense content surrounded by less compact and less dense matrix material (Dvorak and Monahan-Earley, 1995h). The pancreatic islet cells which contain these granules secrete glucagon, and patients with elevated blood sugar can express such pancreatic islet cell tumors, composed of cells that are filled with alpha granules. These distinctive granules were labeled with the R-G method (Fig. 15C). Medullary carcinomas of the thyroid are familial tumors which originate from the calcitonin-secreting "C" cell of the thyroid gland (Dvorak and Monahan-Earley, 1995a,b,d,f). Patients with these malignant neoplasms express the many consequences of elevated serum calcium levels induced by their secretory product, calcitonin. Tumor cells characteristically contain small secretory granules analogous to those in thyroid C cells (Dvorak and Monahan-Earley, 1995a, b, d,f). R-G binds to these calcitonin secretory granules (Fig. 15D).

Pituitary adenomas originate from the various endocrine secretory cells which comprise the anterior compartment of this organ (Dvorak and Monahan-Earley, 1992b,c). For example, chromophobe adenomas, containing prolactin-secreting cells, occur in patients who demonstrate clinical evidence of elevated prolactin secretion, such as amenorrhea and galactorrhea (Dvorak and Monahan-Earley, 1992c). These anterior pituitary endocrine cells have small secretory granules which were labeled with R-G both in their intracytoplasmic location and after extrusion of membrane-free granules to the cell's exterior (Fig. 15E,F). Extensive arrays of RER also characterize these cells; the attached

ribosomes bound R-G as well (Fig. 15E,F). Isolated rat pituitary prolactin secretory granules have been shown to incorporate radiolabeled sulfur and to contain a mixture of sulfated proteoglycans (Giannattasio and Zanini, 1976); thus, it is possible that the observed R-G binding to these granules in humans is to proteoglycans in the granules, whereas the ribosomal label is to RNA in the same cells (Fig. 15E,F).

Another functional pituitary adenoma, the eosinophilic adenoma, secretes growth hormone, which results in the clinical syndrome called acromegaly (Dvorak and Monahan-Earley, 1992b). The adenoma

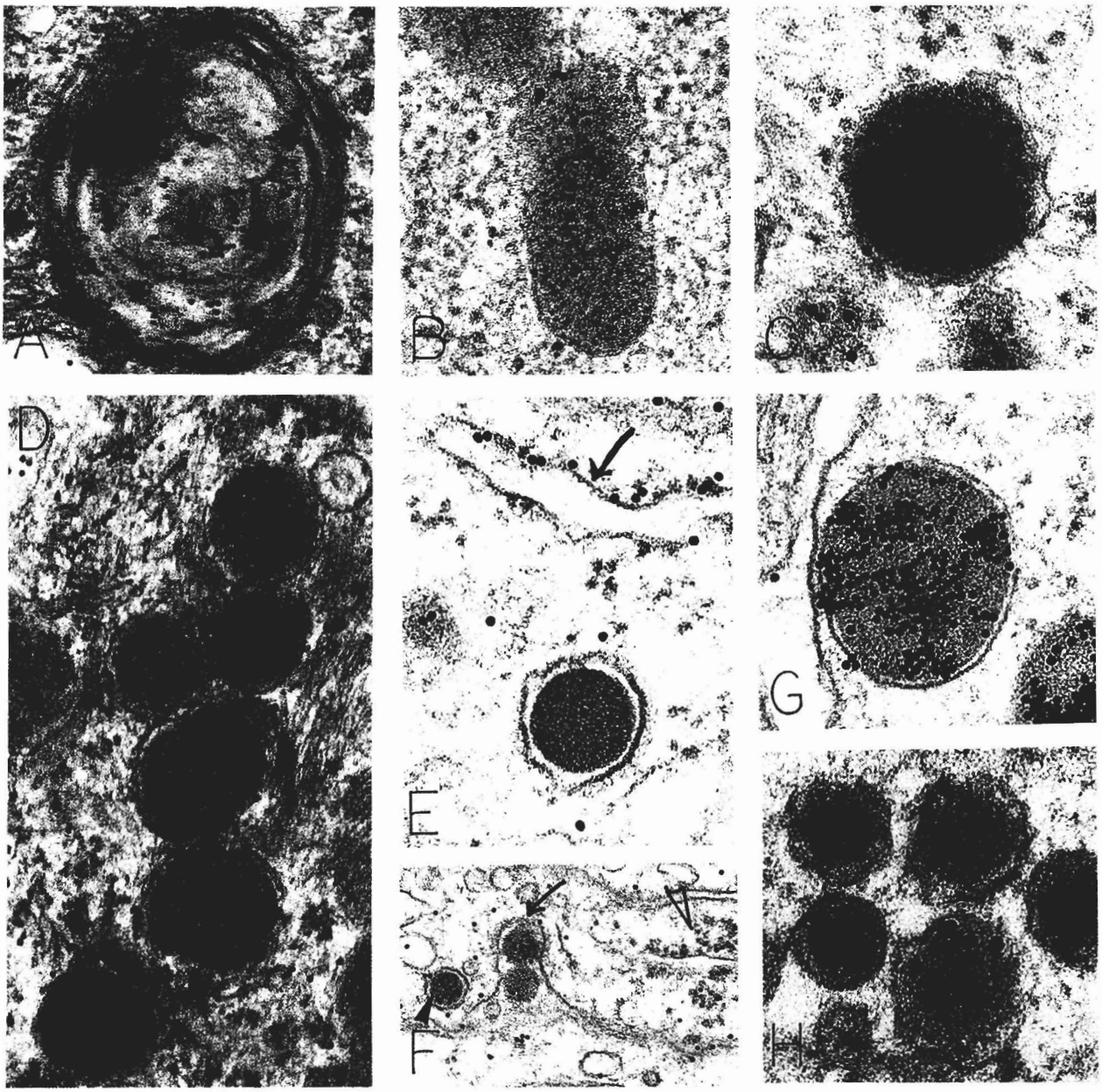

Fig. 15. R-G preparations of secretory granules in human cells. In **(A)**, a lamellar body (known to store surfactant) in a type II alveolar epithelial secretory cell from a lung biopsy shows R-G binding; in **(B)**, a Weibel-Palade body (secretory granular structures that are distinctive for endothelial cells and known to contain von Willebrand factor) binds R-G; in **(C)**, an alpha granule, in a glucagon-secreting pancreatic islet cell tumor (glucagonoma), binds R-G; in **(D)**, secretory granules in a calcitonin-secreting medullary carcinoma of the thyroid bind R-G; in **(E, F)**, prolactin-secreting cells in a chromophobe adenoma of the pituitary bind R-G. The small cytoplasmic secretory granule and ribosomes attached to the RER (arrow) all are labeled in panel E; and, in panel F, intracytoplasmic (black arrowhead) and membrane-free, secreted extracellular granules (arrow) all are labeled with R-G. The open arrowhead indicates R-G-labeled ribosomes on the RER. The growth hormone-secreting, acidophilic pituitary adenoma in a patient with acromegaly displays R-G binding to secretory granules in **(G)**; in **(H)**, the electron-dense granules, typical for a lung carcinoid tumor, are labeled with R-G. A, x 65,000; B, x 107,000; C, x 110,000; D, x 68,000; E, x 99,000; F, x 53,500; G, x 87,500; H, x 149,500

cells in this disorder are characterized by numerous large, electron-dense secretory granules (Dvorak and Monahan-Earley, 1992b). These secretory granules also bound R-G (Fig. 15G).

Carcinoid tumors arise from neuroendocrine cells in many locations (Dvorak and Monahan-Earley, 1992a,g-k). They characteristically are composed of cells which contain varying numbers of variably sized and shaped electron-dense secretory granules. Sometimes, such granules are sufficiently distinctive to allow one to deduce the original sites of metastatic tumors, an exercise for which electron microscopy is essential. Carcinoid tumors of the respiratory system contain numerous small, round electron-dense granules (Dvorak and Monahan-Earley, 1992h-k); these were labeled with R-G (Fig. 15H). Carcinoid tumors arising in the ileum contain secretory granules which have considerable shape and size heterogeneity (Dvorak and Monahan-Earley, 1992a). These granules also bound R-G (data not shown). Carcinoid tumors arising in the ileum contain secretory granules which have considerable shape and size heterogeneity (Dvorak and Monahan-Earley, 1992a). These granules also bound R-G (data not shown). Carcinoid tumors arising in the gastric epithelium can have concentric, thick electron-dense threads and particles (Fig. 16) reminiscent of basophils and mast cells in different species; these granules also bound R-G (Fig. 16A). Control sections stained with bovine serum albumin-gold did not bind this reagent (Fig. 16B).

Altogether, this survey provides extensive evidence for R-G labeling of membrane-bound granules in secretory cells of diverse origin in humans.

18. Ribonuclease-gold labels lysosomes in human tissue macrophages

Human peripheral blood monocytes (Kolset et al., 1983) and peritoneal macrophages (Kolset, 1986), when placed in short-term cultures, synthesize CS proteoglycan with a high sulfate content (Kolset et al., 1983; Kolset, 1986). Sulfated proteoglycans, such as heparin and CS, inhibit lysosomal enzymes at low pH levels. They are regularly present in lysosomes within leukocytes (Avila and Convit, 1976), suggesting a possible functional role for these proteoglycans in lysosome biology. Also, macrophages are avid phagocytes which can internalize and sequester materials such as proteoglycans (Fabian et al., 1978), Charcot-Leyden crystal protein (released from eosinophils [Dvorak et al., 1990]), and RNA-containing cellular debris, within their phagolysosomes.

Lysosomes, membrane-bound, electron-dense cytoplasmic granules of varying size, shape and contents, characterize the monocyte-macrophage lineage. We found that many of the lysosomes in interstitial macrophages in human disease bound the R-G reagent (Fig. 17). While we think it is most probable that the sulfated

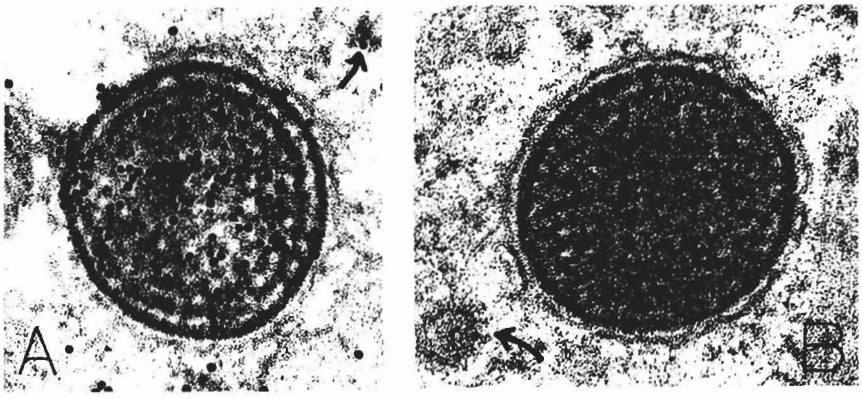

Fig. 16. Secretory granules in a gastric carcinoid tumor show electron-dense concentric threads and particles that label with the R-G method **(A)** but do not bind BSA-gold **(B)**. Cytoplasmic free polysomes bind R-G in (A) (arrow); the arrow in (B) illustrates a typical coated vesicle in this tumor cell. A, x 83,000; B, x 84,000

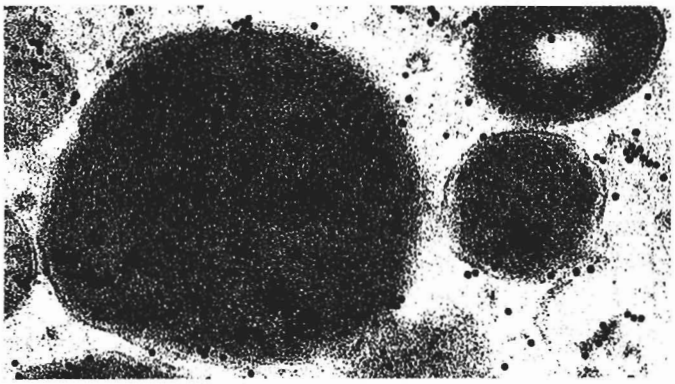

Fig. 17. Lysosomes in macrophages from a biopsy of a patient with interstitial pulmonary fibrosis are labeled with gold particles using the R-G method. x 63,500

proteoglycans in these organelles are responsible for this binding, it is also possible that phagocytosed, RNA-containing organelles in phagolysosomes could contribute to the R-G binding to these organelles in ultrastructural samples.

19. Ribonuclease-gold labels extracellular materials

Extracellular matrix tissue components are constituted of numerous structurally identifiable materials, such as basal lamina and interstitial collagen, in all organs, and cross-linked fibrin in some diseased tissues. We noted that human biopsies, prepared using the R-G method, often had some components of the extracellular tissue that were regularly decorated with gold, whereas others were not. For example, typical interstitial collagen fibrils, either individually distributed or in fascicles of fibrils, bound R-G on their surfaces,

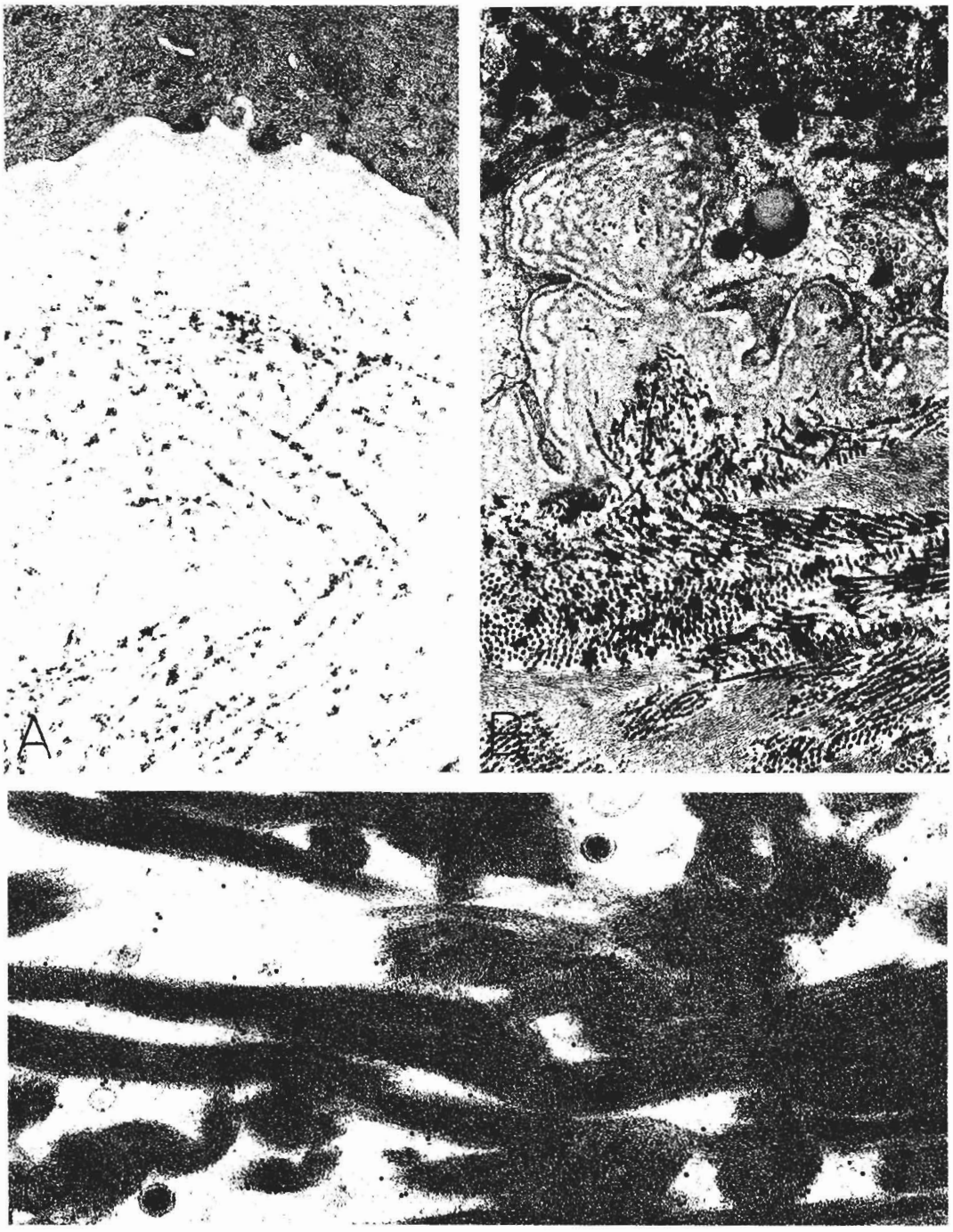

Fig. 18. R-G preparations of tumor stroma from patients with fibroadenoma of the breast **(A, B)** and carcinoid tumor of the lung **(C)**. Epithelial tumor cells are present at the top in panels A and B. They are bounded inferiorly by basal lamina arrays that do not bind R-G. Beneath the negative basal lamina are individual bands (A) and fascicles (B) of interstitial collagen that are stained with R-G (A, B). Panel C illustrates elongated strands of polymerized fibrin with typical periodicity. Note that fibrin binds R-G, whereas the intervening interstitial tissue is devoid of bound gold. A, x 31,000; B, x 15,000; C, x 45,000

whereas neither the lamina densa nor the lamina rara of basal lamina was so-labeled (Fig. 18A,B). Cross-linked fibrin forms in the interstitium of diseased tissue as a consequence of enhanced vessel permeability (Dvorak et al., 1997) and often marks the earliest stage of stroma formation in tumors (Dvorak, 1986; Dvorak et al., 1997). The provisional matrix formed by the fibrin is later replaced by extensive deposits of collagen, a process termed fibrosis. When such extracellular fibrin deposits were present, they too were decorated by the R-G reagent (Fig. 18C).

The known substrate for ribonuclease, RNA, is an intracellular material and generally would not be expected to be present in normal extracellular tissues. Proteoglycans, however, are well-known components of the normal extracellular matrix (Hardingham and Fosang, 1992). The ultrastructural appearance of proteoglycans as electron-dense granules of ~40 nm in diameter, closely associated with the external surfaces of interstitial collagen fibrils (Dell'Orbo et al., 1995), corresponds precisely to the binding localization of R-G. Therefore, in this instance, it seems likely that the R-G reagent is imaging proteoglycan granules in this location.

20. Ribonuclease-gold labels other cellular organelles

We noted other cellular organelles in a wide variety of cells examined with the R-G method that bound this reagent. Although the basis for this binding is not known, the organelles imaged are sufficiently unique that we record some of these findings here (Figs. 19, 20). In addition to the binding of R-G to individual polysome clusters and single ribosomes (Figs. 19, 20A,B), cellular organelles in the same sections that bound R-G included intercellular epithelial junctions (Fig. 19A), centrioles and Golgi area vesicles (Fig. 19B), endothelial cell plasmalemmal vesicles and diaphragms (Fig. 20A,B), endothelial cell vesiculo-vacuolar organelle (VVO) stomata (Dvorak et al., 1996a; Feng et al., 1996) (Fig. 20C), and fenestrated endothelial cell fenestral diaphragms (Fig. 20D).

Centrioles function in microtubule nucleation to promote microtubule growth from cellular tubulin, and they duplicate during each cell division in mitosis (Dictenberg et al., 1998; Tassin et al., 1998). These functions are found in all nucleated cells. Whether RNA, the known substrate for R-G (Bendayan, 1981), or

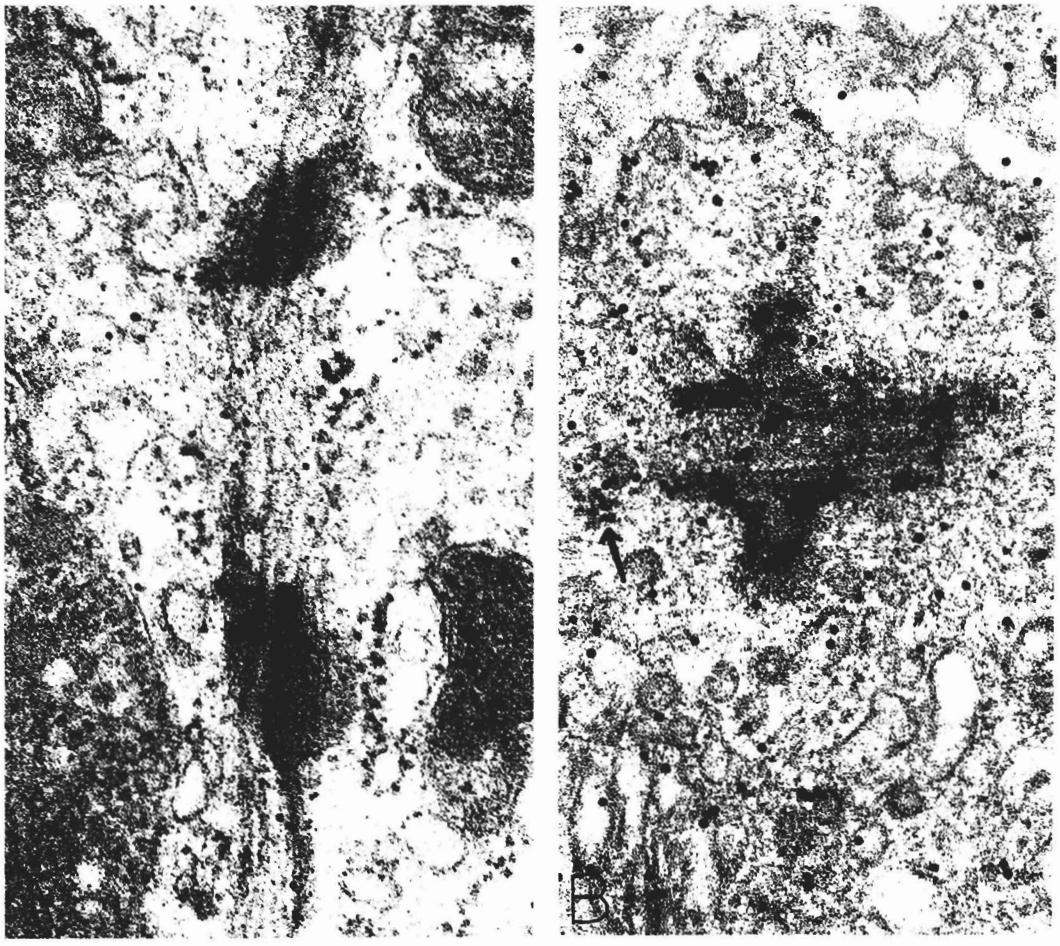

Fig. 19. R-G preparations of epithelial cells in a human breast fibroadenoma **(A)** and the centriole in an eosinophilic myelocyte from the bone marrow of a guinea pig **(B)**. In (A), aside from some labeled cytoplasmic ribosomes, most of the R-G is bound to the intercellular junctions between two epithelial adenoma cells. In (B), the centriole is heavily labeled with R-G. Some gold particles are bound to Golgi vesicles surrounding the centriole as well as to cytoplasmic ribosomes (arrow). A, x 72,000; B, x 90,000

proteoglycans, which bind R-G based on enzyme inhibition properties (Dvorak and Morgan, 1998a, 1998b, 1999), are present in centrosomes is not known. Novel γ-tubulin binding proteins (Tassin et al., 1998), γ-tubulin and pericentrin (Dictenberg et al., 1998) are located in centrosomes. As isolated preparations of

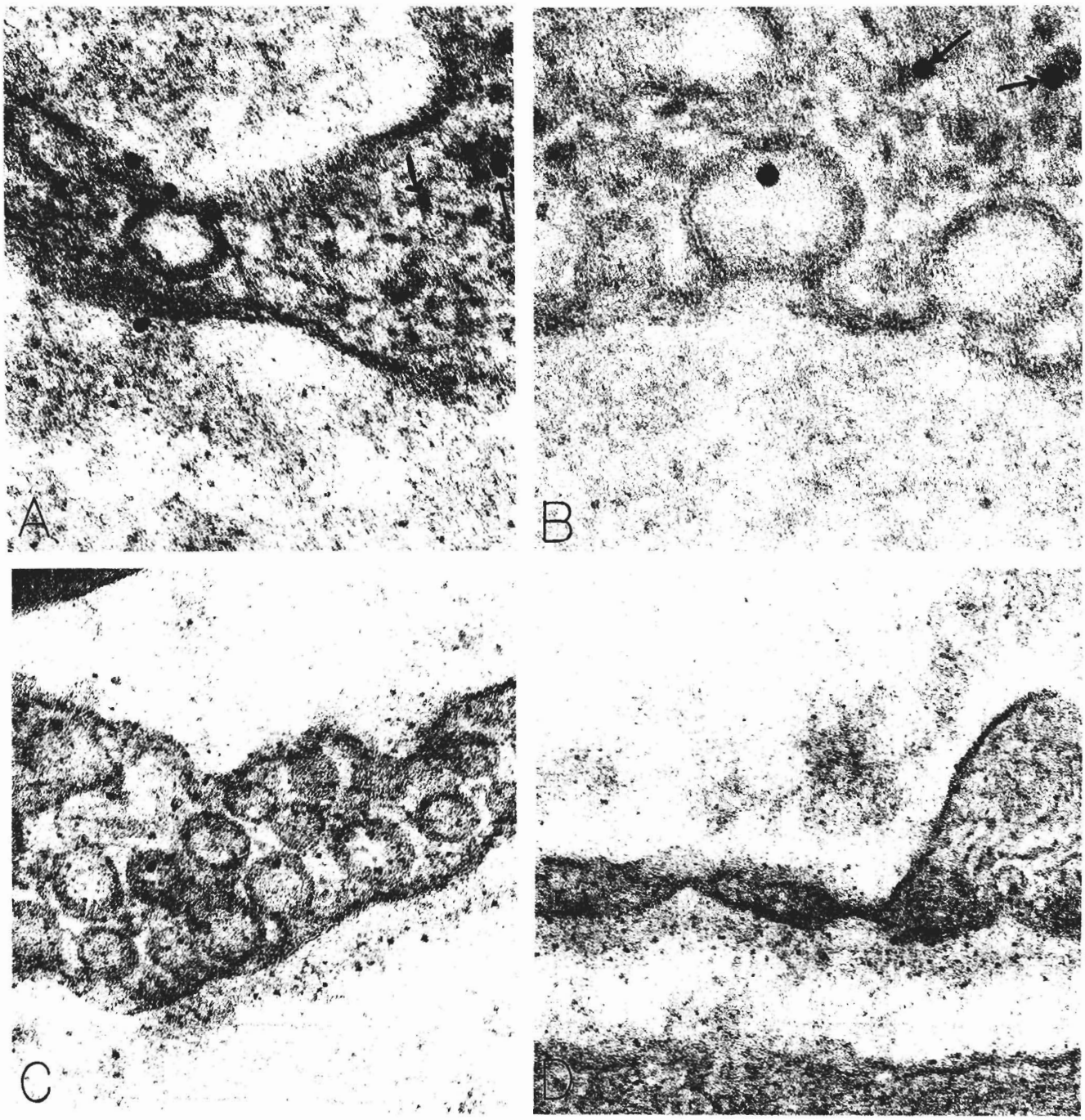

Fig. 20. R-G preparations of endothelial cells in a human breast fibroadenoma. These high magnification micrographs illustrate R-G label associated with individual cytoplasmic ribosomes (arrows in A, B) and with individual structures typical of endothelial cells (A-D). In (A-D), the vascular lumen is at the top of each photograph. In **(A)**, R-G binds to the luminal plasma membrane adjacent to a caveola and to the diaphragm closing this organelle on the luminal surface. The abluminal plasma membrane also binds a gold particle. In **(B)**, the gold label is within a stomatal opening of a caveola that is closed with a diaphragm at the abluminal plasmalemmal surface. In **(C)**, a collection of vesicles comprising a VVO within the endothelial cytoplasm shows binding of R-G to the electron-lucent stomata of one vesicle. In **(D)**, in a portion of fenestrated endothelium, a single R-G particle is present in the center of a fenestral diaphragm. A, x 170,000; B, x 246,500; C, x 122,500; D, x 109,000

centrosomes (Tassin et al., 1998) are further characterized, the basis for binding of R-G to these unique structures may be clarified.

Caveolae (Schnitzer et al., 1995a,b) and VVOs (Dvorak et al., 1996a; Feng et al., 1996), located in endothelial cells, also bound R-G. In high magnification images, the gold binding could be localized to individual components of these unique organelles (Fig. 20). For example, the diaphragms closing the fenestrae of fenestrated endothelium bound R-G (Fig. 20D). These structures (as postulated by several investigators) may be composed of proteoglycans (Clementi and Palade, 1969; Simionescu et al., 1981, 1982; Bankston and Milici, 1983; Rostgaard and Qvortrup, 1997), providing a possible basis for the binding of R-G to them. Little is known regarding the biochemical composition of individual caveolar components, whereas isolated, purified preparations of caveolae are now being defined biochemically (Schnitzer et al., 1995a,b). VVOs are complex collections of connected vesicles and vacuoles that permeabilize venular endothelium (Dvorak et al., 1996a; Feng et al., 1996). We have noted that stomata, identical to those in caveolae, characterize the individual components of VVOs throughout the venular endothelial cytoplasm (Dvorak et al., 1996a). Furthermore, using pre-embedding immunocyto-chemistry, we have localized vascular permeability factor (VPF) (a.k.a. vascular endothelial growth factor [VEGF]) to those stomata, as well as to the VVOs generally, in tumor vasculature which is bathed in VPF/VEGF (Qu-Hong et al., 1995). Whether this unique cytokine is bound to its receptors in this location is not yet known, but it is known that VPF/VEGF binds to heparin (Dvorak et al., 1995, 1997; Brown et al., 1997). Therefore, the stomata and/or their diaphragms may contain heparin which serves to bind R-G in this location.

21. Concluding remarks

Enzyme-gold electron microscopic cytochemistry was initiated when enzyme-gold complexes were used to localize nucleic acids (Bendayan, 1981). This seminal study led to the development and use of a large number of specific enzyme-gold procedures for use in electron microscopy. A special advantage of enzyme-gold electron microscopic cytochemistry is that it works on routinely prepared samples without loss of image quality.

A wider application of the use of enzyme-gold cytochemistry was realized when the inhibitory property of heparin for RNase was utilized to specifically label heparin in human mast cell granules (Dvorak and Morgan, 1998a). This property was extended to the identification of another proteoglycan, chondroitin sulfate (CS), in various cells known to contain CS in the absence of heparin. These cells and sites include guinea pig and human basophil granules, bone marrow-derived, cultured, immature mouse mast cell granules, eosinophil, neutrophil and platelet secretory granules, cloned mouse large granular lymphocyte granules, and Kurloff bodies in guinea pig Kurloff cells.

A survey was undertaken to examine secretory cells of wide origin to determine whether other secretory granule proteoglycans could be imaged with the R-G reagent. These studies, conducted primarily in human biopsies, revealed that secretory granules in type II alveolar pneumocytes, endothelial cells, pancreatic acinar and islet cells, thyroid C cells, functional pituitary adenomas, and carcinoid tumors were labeled with R-G. None of these structures contain heparin, but many are known to contain a mixture of proteoglycans.

The RNA substrate for R-G was also regularly imaged in organelles known to contain RNA in all samples examined, thereby corroborating the original use for this enzyme-gold cytochemical procedure.

Proteoglycan imaging with R-G was useful for determining the changing ultrastructural distributions of proteoglycans in cell maturation, secretion, and recovery from secretion. Specifically, these developmental and functional programs were examined in human mast cells (Dvorak and Morgan, 1999) and guinea pig basophils.

Additional substructural organelles were found to bind R-G. In some cases, the binding probably also is to proteoglycans thought to be associated with these structures. Altogether, these findings document a wider application for R-G cytochemistry, one that includes imaging of proteoglycans as well as the expected substrate, RNA.

Acknowledgements. This work was supported by N.I.H. Grant AI-33372 and by the Lillian Gong Memorial Research Fund. We thank Peter K. Gardner for editorial assistance in the preparation of the manuscript, and Patricia Fox, Linda Letourneau, Kathryn Pyne, Karen Bryan and Tracy Sciuto for expert photographic assistance.

References

Anderson N.G. and Wilbur K.M. (1951). Studies on isolated cell components. II. The release of a nuclear gel by heparin. J. Gen. Physiol. 34, 647-656.

Avila J.L. and Convit J. (1975). Inhibition of leucocytic lysosomal enzymes by glycosaminoglycans *in vitro*. Biochem. J. 152, 57-64.

Avila J.L. and Convit J. (1976). Physicochemical characteristics of the glycosaminoglycan-lysosomal enzyme interaction *in vitro*. A model of control of leucocytic lysosomal activity. Biochem. J. 160, 129-136.

Bankston P.W. and Milici A.J. (1983). A survey of the binding of polycationic ferritin in several fenestrated capillary beds: Indication of heterogeneity in the luminal glycocalyx of fenestral diaphragms. Microvasc. Res. 29, 36-48.

Bendayan M. (1981). Ultrastructural localization of nucleic acids by the use of enzyme-gold complexes. J. Histochem. Cytochem. 29, 531-541.

Bendayan M. (1982). Ultrastructural localization of nucleic acids by the use of enzyme-gold complexes: Influence of fixation and embedding. Biol. Cell 43, 153-156.

Bendayan M. (1984). Enzyme-gold electron microscopic cytochemistry: A new affinity approach for the ultrastructural localization of

macromolecules. J. Electron Microsc. Tech. 1, 349-372.

Bendayan M. (1985). The enzyme-gold technique: A new cytochemical approach for the ultrastructural localization of macromolecules. In: Techniques in Immunocytochemistry. Bullock C.R. and Petrusz P. (eds). Vol. 3. Academic Press, Inc. London. pp 179-201.

Bendayan M. (1989). The enzyme-gold cytochemical approach: A review. In: Colloidal gold. Principles, methods and applications. Hayat M.A. (ed). Vol. 2. Academic Press, Inc. San Diego, CA. pp 117-147.

Bendayan M. and Benhamou N. (1987). Ultrastructural localization of glucoside residues on tissue sections by applying the enzyme-gold approach. J. Histochem. Cytochem. 35, 1149-1155.

Bhavanandan V.P. and Davidson E.A. (1975). Mucopolysaccharides associated with nuclei of cultured mammalian cells. Proc. Natl. Acad. Sci. USA 72, 2032-2036.

Brooks E.M. and Binnington K.C. (1989). Gold labeling with wheat germ agglutinin and RNAse on osmicated tissue embedded in epoxy resin. J. Histochem. Cytochem. 37, 1557-1561.

Brown L.F., Detmar M., Claffey K., Nagy J.A., Feng D., Dvorak A.M. and Dvorak H.F. (1997). Vascular permeability factor/vascular endothelial growth factor: A multifunctional angiogenic cytokine. In: Regulation of angiogenesis. Goldberg I.D. and Rosen E.M. (eds). Birkhäuser Publishing, Ltd. Basel. pp 233-269.

Busch S.J., Martin G.A., Barnhart R.L., Mano M., Cardin A.D. and Jackson R.L. (1992). *Trans*-repressor activity of nuclear glycosaminoglycans on Fos and Jun/AP-1 oncoprotein-mediated transcription. J. Cell Biol. 116, 31-42.

Bussolati G. and Gugliotta P. (1983). Nonspecific staining of mast cells by avidin-biotin-peroxidase complexes (ABC). J. Histochem. Cytochem. 31, 1419-1421.

Carlson S.S. and Wight T.N. (1987). Nerve terminal anchorage protein 1 (TAP-1) is a chondroitin sulfate proteoglycan: Biochemical and electron microscopic characterization. J. Cell Biol. 105, 3075-3086.

Charest P.M., Bergeron F. and Lafontaine J.G. (1985). Ultrastructural localization of DNA and RNA in *Allium porrum* interphase cells by means of nuclease-gold complexes. Histochem. J. 17, 957-966.

Cheniclet C. and Bendayan M. (1990). Comparative pyrimidine- and purine-specific RNAse-gold labeling on pancreatic acinar cells and isolated hepatocytes. J. Histochem. Cytochem. 38, 551-562.

Cheniclet C. and Carde J.-P. (1987). Ultrastructural localization of RNAs in plastids with an RNase-gold method. Biol. Cell 59, 79-88.

Chirgwin J.M., Przybyla A.E., MacDonald R.J. and Rutter W.J. (1979). Isolation of biologically active ribonucleic acid from sources enriched in ribonuclease. Biochemistry 18, 5294-5299.

Clementi F. and Palade G.E. (1969). Intestinal capillaries. I. Permeability to peroxidase and ferritin. J. Cell Biol. 41, 33-58.

Craig S.S., Irani A.-M.A., Metcalfe D.D. and Schwartz L.B. (1993). Ultrastructural localization of heparin to human mast cells of the MC_{TC} and MC_T types by labeling with antithrombin III-gold. Lab. Invest. 69, 552-561.

Dean M.F. and Muir H. (1970). The characterization of a protein-polysaccharide isolated from Kurloff cells of the guinea pig. Biochem. J. 118, 783-790.

Dell'Orbo C., De Luca G., Gioglio L., Quacci D. and Soldi C. (1995). The role of proteoglycans in maintaining collagen fibril morphology. Histol. Histopathol. 10, 583-588.

Dictenberg J.B., Zimmerman W., Sparks C.A., Young A., Vidair C., Zheng Y., Carrington W., Fay F.S. and Doxsey S.J. (1998). Pericentrin and γ-tubulin form a protein complex and are organized into a novel lattice at the centrosome. J. Cell Biol. 141, 163-174.

Dvorak A.M. (1978). Biology and morphology of basophilic leukocytes. In: Immediate hypersensitivity - modern concepts and developments. Bach M.K. (ed). In the series Immunology - Volume 7. Marcel Dekker, Inc. New York. pp 369-405.

Dvorak A.M. (1987). Monograph - Procedural guide to specimen handling for the ultrastructural pathology service laboratory. J. Electron Microsc. Tech. 6, 255-301.

Dvorak A.M. (1988). Morphologic and immunologic characterization of human basophils, 1879 to 1985. Riv. Immunol. Immunofarmacol. 8, 50-83.

Dvorak A.M. (1992). Basophils and mast cells: Piecemeal degranulation in situ and ex vivo: A possible mechanism for cytokine-induced function in disease. In: Granulocyte responses to cytokines. Basic and clinical research. Coffey R.G. (ed). Marcel Dekker, Inc. New York. pp 169-271.

Dvorak A.M. (1996). Weibel-Palade body. Blood 87, 4909.

Dvorak A.M. (1998). Cell biology of the basophil. Int. Rev. Cytol. 180, 87-236.

Dvorak A.M. and Dvorak H.F. (1993). Cutaneous basophil hypersensitivity - A 20-year perspective, 1970-1990. In: Immunopharmacology of mast cells and basophils. Foreman J.C. (ed). In the series. The handbook of immunopharmacology (Page C., series ed). Academic Press. London. pp 153-180.

Dvorak A.M. and Galli S.J. (1987). Antigen-induced, IgE-mediated degranulation of cloned immature mast cells derived from normal mice. Am. J. Pathol. 126, 535-545.

Dvorak A.M. and Monahan R.A. (1985). Guinea pig bone marrow basophilopoiesis. J. Exp. Pathol. 2, 13-24.

Dvorak A.M. and Monahan-Earley R.A. (1992a). Case 8: Fatigue, flushing and abdominal lymphadenopathy in a 58-year-old man. Metastatic carcinoid tumor of midgut origin. In: Diagnostic ultrastructural pathology I. A text-atlas of case studies illustrating the correlative clinical-ultrastructural pathologic approach to diagnosis. CRC Press, Inc. Boca Raton, FL. pp 56-65.

Dvorak A.M. and Monahan-Earley R.A. (1992b). Case 16: Bitemporal visual field defects and increasing shoe, ring and hat size in a 33-year-old woman. Pituitary adenoma, densely granulated, growth hormone cell type (Acromegaly). In: Diagnostic ultrastructural pathology I. A text-atlas of case studies illustrating the correlative clinical-ultrastructural pathologic approach to diagnosis. CRC Press, Inc. Boca Raton, FL. pp 155-158.

Dvorak A.M. and Monahan-Earley R.A. (1992c). Case 18: Amenorrhea and galactorrhea in a 25-year-old woman. Prolactinoma. In: Diagnostic ultrastructural pathology I. A text-atlas of case studies illustrating the correlative clinical-ultrastructural pathologic approach to diagnosis. CRC Press, Inc. Boca Raton, FL. pp 163-170.

Dvorak A.M. and Monahan-Earley R.A. (1992d). Case 21: Rapidly progressive lung disease in a 46-year-old woman with scleroderma. Bronchiolo-alveolar carcinoma. In: Diagnostic ultrastructural pathology I. A text-Atlas of case studies illustrating the correlative clinical-ultrastructural pathologic approach to diagnosis. CRC Press, Inc. Boca Raton, FL. pp 191-198.

Dvorak A.M. and Monahan-Earley R.A. (1992e). Case 22: Neurological findings and loss of consciousness in a previously well 47-year-old woman. Alveolar cell carcinoma of the lung, metastatic to the brain. In: Diagnostic ultrastructural pathology I. A text-atlas of case studies illustrating the correlative clinical-ultrastructural pathologic approach to diagnosis. CRC Press, Inc. Boca Raton, FL. pp 199-207.

Dvorak A.M. and Monahan-Earley R.A. (1992f). Case 24: Chronic cough, dyspnea and bilateral lung infiltrates in a 38-year-old man. Pulmonary alveolar proteinosis. In: Diagnostic ultrastructural pathology I. A text-atlas of case studies illustrating the correlative clinical-ultrastructural pathologic approach to diagnosis. CRC Press, Inc. Boca Raton, FL. pp 213-224.

Dvorak A.M. and Monahan-Earley R.A. (1992g). Case 25: Hemoptysis and atelectasis in a 53-year-old woman. Bronchial carcinoid tumor. In: Diagnostic ultrastructural pathology I. A text-atlas of case studies illustrating the correlative clinical-ultrastructural pathologic approach to diagnosis. CRC Press, Inc. Boca Raton, FL. pp 225-230.

Dvorak A.M. and Monahan-Earley R.A. (1992h). Case 26: Slowly enlarging peripheral lung coin lesion in an asymptomatic 62-year-old woman. Peripheral pulmonary carcinoid tumor. In: Diagnostic ultrastructural pathology I. A text-atlas of case studies illustrating the correlative clinical-ultrastructural pathologic approach to diagnosis. CRC Press, Inc. Boca Raton, FL. pp 231-237.

Dvorak A.M. and Monahan-Earley R.A. (1992i). Case 27: Cough and peripheral lung nodule in a 52-year-old man. Atypical carcinoid tumor of the lung. In: Diagnostic ultrastructural pathology I. A text-atlas of case studies illustrating the correlative clinical-ultrastructural pathologic approach to diagnosis. CRC Press, Inc. Boca Raton, FL. pp 238-249.

Dvorak A.M. and Monahan-Earley R.A. (1992j). Case 28: Abnormal chest x-ray in a healthy 37-year-old woman. Atypical carcinoid tumor of the lung. In: Diagnostic ultrastructural pathology I. A text-atlas of case studies illustrating the correlative clinical-ultrastructural pathologic approach to diagnosis. CRC Press, Inc. Boca Raton, FL. pp 250-255.

Dvorak A.M. and Monahan-Earley R.A. (1992k). Case 29: Abnormal chest x-ray in a healthy 50-year-old man. Atypical carcinoid tumor of the lung. In: Diagnostic ultrastructural pathology I. A text-atlas of case studies illustrating the correlative clinical-ultrastructural pathologic approach to diagnosis. CRC Press, Inc. Boca Raton, FL. pp 256-260.

Dvorak A.M. and Monahan-Earley R.A. (1995a). Case 8: Family history of multiple endocrine neoplasia in an asymptomatic 26-year-old man. Medullary carcinoma of the thyroid. In: Diagnostic ultrastructural pathology. III. A Text-atlas of case studies emphasizing endocrine and hematopoietic systems. CRC Press, Inc. Boca Raton, FL. pp 87-95.

Dvorak A.M. and Monahan-Earley R.A. (1995b). Case 9: Neck mass in a 52-year-old woman with multiple endocrine neoplasia. Medullary carcinoma of the thyroid. In: Diagnostic ultrastructural pathology. III. A text-atlas of case studies emphasizing endocrine and hematopoietic systems. CRC Press, Inc. Boca Raton, FL. pp 96-109.

Dvorak A.M. and Monahan-Earley R.A. (1995c). Case 10: Progressive cough and shortness of breath in a 34-year-old man. Diffuse interstitial fibrosis and mast cell hyperplasia of the lung consistent with hypersensitivity pneumonitis. In: Diagnostic ultrastructural pathology. II. A text-atlas of case studies emphasizing respiratory and nervous systems. CRC Press, Inc. Boca Raton, FL. pp 142-163.

Dvorak A.M. and Monahan-Earley R.A. (1995d). Case 10: Neck mass in a 35-year-old man with multiple endocrine neoplasia. Medullary carcinoma of the thyroid. In: Diagnostic ultrastructural pathology. III. A text-atlas of case studies emphasizing endocrine and hematopoietic systems. CRC Press, Inc. Boca Raton, FL. pp 110-127.

Dvorak A.M. and Monahan-Earley R.A. (1995e). Case 11: Cough, heavy smoking history, abnormal lung x-ray, and a strong family history for neoplasia in a 63-year-old woman. Bronchiolo-alveolar carcinoma. In: Diagnostic ultrastructural pathology. II. A text-atlas of case studies emphasizing respiratory and nervous systems. CRC Press, Inc. Boca Raton, FL. pp 164-172.

Dvorak A.M. and Monahan-Earley R.A. (1995f). Case 11: Paroxysms of headache, sweating, and hypertension in a 56-year-old woman. Bilateral pheochromocytomas and medullary carcinoma of the thyroid (multiple endocrine neoplasia). In: Diagnostic ultrastructural pathology. III. A text-atlas of case studies emphasizing endocrine and hematopoietic systems. CRC Press, Inc. Boca Raton, FL. pp 128-155.

Dvorak A.M. and Monahan-Earley R.A. (1995g). Case 12: Lung lesion in a 52-year-old woman with a past history of breast and lung cancer. Bronchiolo-alveolar carcinoma. In: Diagnostic ultrastructural pathology. II. A text-Atlas of case studies emphasizing respiratory and nervous systems. CRC Press, Inc. Boca Raton, FL. pp 173-184.

Dvorak A.M. and Monahan-Earley R.A. (1995h). Case 17: Elevated serum gastrin in a 32-year-old woman with the multiple endocrine neoplasia syndrome. Glucagonoma. In: Diagnostic ultrastructural pathology. III. A text-atlas of case studies emphasizing endocrine and hematopoietic systems. CRC Press, Inc. Boca Raton, FL. pp 237-259.

Dvorak A.M. and Monahan-Earley R.A. (1995i). Case 20: Thrombocytopenia in a 32-year-old woman. Bernard-Soulier syndrome. In: Diagnostic ultrastructural pathology. III. A text-atlas of case studies emphasizing endocrine and hematopoietic systems. CRC Press, Inc. Boca Raton, FL. pp 287-314.

Dvorak A.M. and Monahan-Earley R.A. (1995j). Case 21: Thrombocytopenia in a 15-year-old male. Gray platelet syndrome. In: Diagnostic ultrastructural pathology. III. A text-atlas of case studies emphasizing endocrine and hematopoietic systems. CRC Press, Inc. Boca Raton, FL. pp 315-366.

Dvorak A.M. and Morgan E.S. (1996). Ultrastructural detection of histamine in human mast cells developing from cord blood cells cultured with human or murine recombinant c-kit ligands. Int. Arch. Allergy Immunol. 111, 238-244.

Dvorak A.M. and Morgan E.S. (1997). Diamine oxidase-gold enzyme-affinity ultrastructural demonstration that human gut mucosal mast cells secrete histamine by piecemeal degranulation in vivo. J. Allergy Clin. Immunol. 99, 812-820.

Dvorak A.M. and Morgan E.S. (1998a). Ribonuclease-gold labels heparin in human mast cell granules: New use for an ultrastructural enzyme affinity technique. J. Histochem. Cytochem. 46, 695-706.

Dvorak A.M. and Morgan E.S. (1998b). Ribonuclease-gold labels chondroitin sulfate in guinea pig basophil granules. Histochem. J. 30, 1-6.

Dvorak A.M. and Morgan E.S. (1999). Ribonuclease-gold ultrastructural localization of heparin in isolated human lung mast cells stimulated to undergo anaphylactic degranulation and recovery *in vitro* Clin. Exp. Allergy (in press).

Dvorak A.M., Dvorak H.F. and Karnovsky M.J. (1972). Cytochemical localization of peroxidase activity in the developing erythrocyte. Am. J. Pathol. 67, 303-326.

Dvorak A.M., Galli S.J., Morgan E., Galli A.S., Hammond M.E. and Dvorak H.F. (1981a). Anaphylactic degranulation of guinea pig basophilic leukocytes. I. Fusion of granule membranes and cytoplasmic vesicles: Formation and resolution of degranulation sacs. Lab. Invest. 44, 174-191.

Dvorak A.M., Osage J.E., Dvorak H.F. and Galli S.J. (1981b). Surface

membrane alterations in guinea pig basophils undergoing anaphylactic degranulation. A scanning electron microscopic study. Lab. Invest. 45, 58-66.

Dvorak A.M., Galli S.J., Morgan E., Galli A.S., Hammond M.E. and Dvorak H.F. (1982). Anaphylactic degranulation of guinea pig basophilic leukocytes. II. Evidence for regranulation of mature basophils during recovery from degranulation *in vitro*. Lab. Invest. 46, 461-475.

Dvorak A.M., Galli S.J., Marcum J.A., Nabel G., Der Simonian H., Goldin J., Monahan R.A., Pyne K., Cantor H., Rosenberg R.D. and Dvorak H.F. (1983). Cloned mouse cells with natural killer function and cloned suppressor T cells express ultrastructural and biochemical features not shared by cloned inducer T cells. J. Exp. Med. 157, 843-861.

Dvorak A.M., Colvin R.B. and Monahan R.A. (1985). Immunoferritin electron microscopic studies with antibasophil serum of guinea pig basophil degranulation and regranulation *in vitro*. Clin. Immunol. Immunopathol. 37, 63-76.

Dvorak A.M., Monahan-Earley R.A., Dvorak H.F. and Galli S.J. (1987). Ultrastructural cytochemical and autoradiographic demonstration of nonspecific esterase(s) in guinea pig basophils. J. Histochem. Cytochem. 35, 351-360.

Dvorak A.M., Weller P.F., Monahan-Earley R.A., Letourneau L. and Ackerman S.J. (1990). Ultrastructural localization of Charcot-Leyden crystal protein (lysophospholipase) and peroxidase in macrophages, eosinophils and extracellular matrix of the skin in the hyper-eosinophilic syndrome. Lab. Invest. 62, 590-607.

Dvorak A.M., McLeod R.S., Onderdonk A., Monahan-Earley R.A., Cullen J.B., Antonioli D.A., Morgan E., Blair J.E., Estrella P., Cisneros R.L., Silen W. and Cohen Z. (1992). Ultrastructural evidence for piecemeal and anaphylactic degranulation of human gut mucosal mast cells *in vivo*. Int. Arch. Allergy Immunol. 99, 74-83.

Dvorak A.M., Morgan E.S., Schleimer R.P. and Lichtenstein L.M. (1993). Diamine oxidase-gold labels histamine in human mast-cell granules: A new enzyme-affinity ultrastructural method. J. Histochem. Cytochem. 41, 787-800.

Dvorak A.M., Morgan E.S., Lichtenstein L.M. and MacGlashan D.W. Jr. (1994a). Activated human basophils contain histamine in cytoplasmic vesicles. Int. Arch. Allergy Immunol. 105, 8-11.

Dvorak A.M., Tepper R.I., Weller P.F., Morgan E.S., Estrella P., Monahan-Earley R.A. and Galli S.J. (1994b). Piecemeal degranulation of mast cells in the inflammatory eyelid lesions of interleukin-4 transgenic mice. Evidence of mast cell histamine release in vivo by diamine oxidase-gold enzyme-affinity ultrastructural cytochemistry. Blood 83, 3600-3612.

Dvorak A.M., MacGlashan D.W. Jr, Morgan E.S. and Lichtenstein L.M. (1995). Histamine distribution in human basophil secretory granules undergoing FMLP-stimulated secretion and recovery. Blood 86, 3560-3566.

Dvorak A.M., Kohn S., Morgan E.S., Fox P., Nagy J.A. and Dvorak H.F. (1996a). The vesiculo-vacuolar organelle (VVO): a distinct endothelial cell structure that provides a transcellular pathway for macromolecular extravasation. J. Leukoc. Biol. 59, 100-115.

Dvorak A.M., MacGlashan D.W. Jr, Morgan E.S. and Lichtenstein L.M. (1996b). Vesicular transport of histamine in stimulated human basophils. Blood 88, 4090-4101.

Dvorak A.M., Morgan E.S., Schleimer R.P. and Lichtenstein L.M. (1996c). Diamine oxidase-gold ultrastructural localization of histamine in isolated human lung mast cells stimulated to undergo anaphylactic degranulation and recovery in vitro. J. Leukoc. Biol. 59, 824-834.

Dvorak A.M., Costa J.J., Morgan E.S., Monahan-Earley R.A. and Galli S.J. (1997). Diamine oxidase-gold ultrastructural localization of histamine in human skin biopsies containing mast cells stimulated to degranulate *in vivo* by exposure to recombinant human stem cell factor. Blood 90, 2893-2900.

Dvorak H.F. (1986). Tumors: Wounds that do not heal. Similarities between tumor stroma generation and wound healing. N. Engl. J. Med. 315, 1650-1659.

Dvorak H.F., Selvaggio S.S., Dvorak A.M., Colvin R.B., Lean D.B. and Rypysc J. (1974). Purification of basophilic leukocytes from guinea pig blood and bone marrow. J. Immunol. 113, 1694-1702.

Dvorak H.F., Orenstein N.S., Dvorak A.M., Hammond M.E., Roblin R.O., Feder J., Schott C.F., Goodwin J. and Morgan E. (1977). Isolation of the cytoplasmic granules of guinea pig basophilic leukocytes: Identification of esterase and protease activities. J. Immunol. 119, 38-46.

Dvorak H.F., Brown L.F., Detmar M. and Dvorak A.M. (1995). Vascular permeability factor/vascular endothelial cell growth factor, microvascular hyperpermeability, and angiogenesis. Am. J. Pathol. 146, 1029-1039.

Dvorak H.F., Brown L.F., Nagy J.A., Feng D. and Dvorak A.M. (1997). Vascular hyperpermeability in tumors and inflammation. In: Vascular endothelium. Physiology, pathology, and therapeutic opportunities. In the series hew Horizon series, Vol. 3. Born G.V.R. and Schwartz C.J. (series eds). F.K. Schattauer Verlagsgesellschaft. Stuttgart. pp 345-354.

Fabian I., Bleiberg I. and Aronson M. (1978). Increased uptake and desulphation of heparin by mouse macrophages in the presence of polycations. Biochim. Biophys. Acta 544, 69-76.

Feng D., Nagy J.A., Hipp J., Dvorak H.F. and Dvorak A.M. (1996). Vesiculo-vacuolar organelles and the regulation of venule permeability to macromolecules by vascular permeability factor, histamine and serotonin. J. Exp. Med. 183, 1981-1986.

Frens G. (1973). Controlled nucleation for the regulation of the particle size in monodisperse gold suspensions. Nature Phys. Sci. 241, 20-22.

Fromme H.G., Buddecke E., Figura K.V. and Kresse H. (1976). Localization of sulfated glycosaminoglycans within cell nuclei by high-resolution autoradiography. Exp. Cell Res. 102, 445-449.

Galli S.J., Orenstein N.S., Gill P.J., Silbert J.E., Dvorak A.M. and Dvorak H.F. (1979). Sulphated glycosaminoglycans synthesised by basophil-enriched human leukaemic granulocytes. In: The mast cell. Its role in health and disease. Pepys J. and Edwards A.M. (eds). Pitman Medical Publishing Company, Ltd. Kent. p 842.

Galli S.J., Dvorak A.M., Ishizaka T., Nabel G., Der Simonian H., Cantor H. and Dvorak H.F. (1982a). A cloned cell with natural killer (NK) function resembles basophils by ultrastructure and expresses IgE receptors. Nature 298, 288-290.

Galli S.J., Dvorak A.M., Marcum J.A., Ishizaka T., Nabel G., Der Simonian H., Pyne K., Goldin J.M., Rosenberg R.D., Cantor H. and Dvorak H.F. (1982b). Mast cell clones: A model for the analysis of cellular maturation. J. Cell Biol. 95, 435-444.

Galli S.J., Dvorak A.M. and Dvorak H.F. (1984). Basophils and mast cells: Morphologic insights into their biology, secretory patterns, and function. In: Mast cell activation and mediator release. Ishizaka K. (ed). Vol. 34 in the series: Progress in allergy. S. Karger. Basel. pp 1-141.

Giannattasio G. and Zanini A. (1976). Presence of sulfated proteoglycans in prolactin secretory granules isolated from the rat pituitary gland. Biochim. Biophys. Acta 439, 349-357.

Greene L.J., Hirs C.H.W. and Palade G.E. (1963). On the protein composition of bovine pancreatic zymogen granules. J. Biol. Chem. 238, 2054-2070.

Hardin J.H. and Spicer S.S. (1971). Ultrastructural localization of dialyzed iron-reactive mucosubstance in rabbit heterophils, basophils, and eosinophils. J. Cell Biol. 48, 368-386.

Hardingham T.E. and Fosang A.J. (1992). Proteoglycans: Many forms and many functions. FASEB J. 6, 861-870.

Hart G.W., Haltiwanger R.S., Holt G.D. and Kelly W.G. (1989). Glycosylation in the nucleus and cytoplasm. Annu. Rev. Biochem. 58, 841-874.

Hastie R. (1974). A study of the ultrastructure of human basophil leukocytes. Lab. Invest. 31, 223-231.

Hay E.D. (1981). Extracellular matrix. J. Cell Biol. 91, 205s-223s.

Holmes D.S., Mayfield J.E., Sander G. and Bonner J. (1972). Chromosomal RNA: Its properties. Science 177, 72-74.

Horn R.G. and Spicer S.S. (1964). Sulfated mucopolysaccharide and basic protein in certain granules of rabbit leukocytes. Lab. Invest. 13, 1-15.

Ishizaka T., Conrad D.H., Huff T.F., Metcalfe D.D., Stevens R.L. and Lewis R.A. (1985). Unique features of human basophilic granulocytes developed in *in vitro* culture. Int. Arch. Allergy Appl. Immunol. 77, 137-143.

Jaques L.B. (1980). Heparins–Anionic polyelectrolyte drugs. Pharmacol. Rev. 31, 99-166.

Kan F.W.K. (1990). High-resolution localization of hyaluronic acid in the golden hamster oocyte-cumulus complex by use of a hyaluronidase-gold complex. Anat. Rec. 228, 370-382.

Kellenberger E., Dürrenberger M., Villiger W., Carlemalm E. and Wurtz M. (1987). The efficiency of immunolabel on Lowicryl sections compared to theoretical predictions. J. Histochem. Cytochem. 35, 959-969.

Kobayashi Y. (1962). Histamine binding by heparin. Arch. Biochem. Biophys. 96, 20-27.

Kolset S.O. (1986). Oversulfated chondroitin sulfate proteoglycan in cultured human peritoneal macrophages. Biochem. Biophys. Res. Commun. 139, 377-382.

Kolset S.O., Kjellén L., Seljelid R. and Lindahl U. (1983). Changes in glycosaminoglycan biosynthesis during differentiation *in vitro* of human monocytes. Biochem. J. 210, 661-667.

Kolset S.O., Mann D.M., Uhlin-Hansen L., Winberg J.-O. and Ruoslahti E. (1996). Serglycin-binding proteins in activated macrophages and platelets. J. Leukoc. Biol. 59, 545-554.

Kronquist K.E., Elmahdy A. and Ronzio R.A. (1977). Synthesis and subcellular distribution of heparan sulfate in the rat exocrine pancreas. Arch. Biochem. Biophys. 182, 188-196.

Lagunoff D. (1974). Analysis of dye binding sites in mast cell granules. Biochemistry 13, 3982-3986.

Lagunoff D., Phillips M. and Benditt E.P. (1961). The histochemical demonstration of histamine in mast cells. J. Histochem. Cytochem. 9, 534-541.

Levine S.P., Knieriem L.K. and Rager M.A. (1990). Platelet factor 4 and the platelet secreted proteoglycan: Immunologic characterization by crossed immunoelectrophoresis. Blood 75, 902-910.

Levitt D. and Ho P.-L. (1983). Induction of chondroitin sulfate proteoglycan synthesis and secretion in lymphocytes and monocytes. J. Cell Biol. 97, 351-358.

Lindahl U. and Höök M. (1978). Glycosaminoglycans and their binding to biological macromolecules. Annu. Rev. Biochem. 47, 385-417.

Linker A. and Hovingh P. (1972). Heparinase and heparitinase from flavobacteria. Methods Enzymol. 28, 902-911.

Login G.R., Galli S.J. and Dvorak A.M. (1992). Immunocytochemical localization of histamine in secretory granules of rat peritoneal mast cells with conventional or rapid microwave fixation and an ultrastructural post-embedding immunogold technique. J. Histochem. Cytochem. 40, 1247-1256.

Londoño I. and Bendayan M. (1988). High-resolution cytochemistry of neuraminic and hexuronic acid-containing macromolecules applying the enzyme-gold approach. J. Histochem. Cytochem. 36, 1005-1014.

MacPherson G.G. (1972). Synthesis and localization of sulphated mucopolysaccharide in megakaryocytes and platelets of the rat, an analysis by electron-microscope autoradiography. J. Cell Sci. 10, 705-717.

McLaren K.M. and Pepper D.S. (1983). The immunoelectronmicroscopic localization of human platelet factor 4 in tissue mast cells. Histochem. J. 15, 795-800.

Meldolesi J., Jamieson J.D. and Palade G.E. (1971). Composition of cellular membranes in the pancreas of the guinea pig. I. Isolation of membrane fractions. J. Cell Biol. 49, 109-129.

Mendelsohn S.L. and Young D.A. (1978). Inhibition of ribonuclease. Efficacy of sodium dodecyl sulfate, diethyl pyrocarbonate, proteinase K and heparin using a sensitive ribonuclease assay. Biochim. Biophys. Acta 519, 461-473.

Metcalfe D.D., Litvin J. and Wasserman S.I. (1982). The isolation, identification and characterization of sulfated glycosaminoglycans synthesized in vitro by human eosinophils. Biochim. Biophys. Acta 715, 196-204.

Metcalfe D.D., Bland C.E. and Wasserman S.I. (1984). Biochemical and functional characterization of proteoglycans isolated from basophils of patients with chronic myelogenous leukemia. J. Immunol. 132, 1943-1950.

Morioka H., Tachibana M., Amagai T. and Suganuma A. (1986). Aminoglycoside binding sites in *Escherichia coli* as revealed by neomycin-gold labeling. J. Histochem. Cytochem. 34, 909-912.

Nabel G., Galli S.J., Dvorak A.M., Dvorak H.F. and Cantor H. (1981). Inducer T lymphocytes synthesize a factor that stimulates proliferation of cloned mast cells. Nature 291, 332-334.

Oliani S.M., Freymüller E., Takahashi H.K. and Straus A.H. (1997). Immunocytochemical localization of heparin in secretory granules of rat peritoneal mast cells using a monoclonal anti-heparin antibody (ST-1). J. Histochem. Cytochem. 45, 231-235.

Olsson I. (1968). Biosynthesis of glycosaminoglycans (mucopolysaccharides) in leukemic myeloid cells. Biochim. Biophys. Acta 165, 324-334.

Olsson I. and Gardell S. (1967). Isolation and characterization of glycosaminoglycans from human leukocytes and platelets. Biochim. Biophys. Acta 141, 348-357.

Olsson I., Gardell S. and Thunell S. (1968). Biosynthesis of glycosaminoglycans (mucopolysaccharides) in human leukocytes. Biochim. Biophys. Acta 165, 309-323.

Orenstein N.S., Galli S.J., Dvorak A.M., Silbert J.E. and Dvorak H.F. (1978). Sulfated glycosaminoglycans of guinea pig basophilic leukocytes. J. Immunol. 121, 586-592.

Orenstein N.S., Galli S.J., Dvorak A.M. and Dvorak H.F. (1981).

Glycosaminoglycans and proteases of guinea pig basophilic leukocytes. In: Biochemistry of the acute allergic reactions: Fourth International Symposium. Becker E.L., Simon A.S. and Austen K.F. (eds). Alan R. Liss, Inc. New York. pp 123-143.

Parmley R.T., Spicer S.S., Komiyama A., Dow L.W. and Austin R.L. (1979). Ultrastructural cytochemistry of basophils in chronic myelocytic leukemia. Exp. Mol. Pathol. 30, 41-54.

Ploton D., Bendayan M. and Adnet J.-J. (1983). Ultrastructural localization of Ag-NOR proteins and nucleic acids in reticulated nucleoli. Biol. Cell 49, 29-34.

Qu-Hong, Nagy J.A., Senger D.R., Dvorak H.F. and Dvorak A.M. (1995). Ultrastructural localization of vascular permeability factor/vascular endothelial growth factor (VPF/VEGF) to the abluminal plasma membrane and vesiculovacuolar organelles of tumor microvascular endothelium. J. Histochem. Cytochem. 43, 381-389.

Rapraeger A.C. and Bernfield M. (1983). Heparan sulfate proteoglycans from mouse mammary epithelial cells. A putative membrane proteoglycan associates quantitatively with lipid vesicles. J. Biol. Chem. 258, 3632-3636.

Reggio H. and Dagorn J.C. (1978). Ionic interactions between bovine chymotrypsinogen A and chondroitin sulfate A.B.C. A possible model for molecular aggregation in zymogen granules. J. Cell Biol. 78, 951-957.

Reggio H.A. and Palade G.E. (1978). Sulfated compounds in the zymogen granules of the guinea pig pancreas. J. Cell Biol. 77, 288-314.

Revell P.A. (1977). The Kurloff cell. Int. Rev. Cytol. 51, 275-314.

Riley J.F. and West G.B. (1953). The presence of histamine in tissue mast cells. J. Physiol. 120, 528-537.

Rossmann P., Matousovic K. and Horacek V. (1982). Protamine-heparin aggregates. Their fine structure, histochemistry, and renal deposition. Virchows Arch. (B) 40, 81-98.

Rostgaard J. and Qvortrup K. (1997). Electron microscopic demonstrations of filamentous molecular sieve plugs in capillary fenestrae. Microvasc. Res. 53, 1-13.

Salmivirta M., Lidholt K. and Lindahl U. (1996). Heparan sulfate: A piece of information. FASEB J. 10, 1270-1279.

Sanyal R.K. and West G.B. (1956). Binding of histamine in mammalian tissues. Nature 170, 1293.

Schick B.P. and Eras J. (1995). Proteoglycans partially co-purify with RNA in TRI Reagent™ and can be transferred to filters by Northern blotting. BioTechniques 18, 574-578.

Schnitzer J.E., McIntosh D.P., Dvorak A.M., Liu J. and Oh P. (1995a). Separation of caveolae from associated microdomains of GPI-anchored proteins. Science 269, 1435-1439.

Schnitzer J.E., Oh P., Jacobson B.S. and Dvorak A.M. (1995b). Caveolae from luminal plasmalemma of rat lung endothelium: Microdomains enriched in caveolin, Ca^{++}-ATPase, and inositol triphosphate receptor. Proc. Natl. Acad. Sci. USA 92, 1759-1763.

Simionescu M., Simionescu N., Silbert J.E. and Palade G.E. (1981). Differentiated microdomains on the luminal surface of the capillary endothelium. II. Partial characterization of their anionic sites. J. Cell Biol. 90, 614-621.

Simionescu M., Simionescu N. and Palade G.E. (1982). Differentiated microdomains on the luminal surface of capillary endothelium: Distribution of lectin receptors. J. Cell Biol. 94, 406-413.

Skutelsky E., Shoichetman T. and Hammel I. (1995). An histochemical approach to characterization of anionic constituents in mast cell secretory granules. Histochem. Cell Biol. 104, 453-458.

Spicer S.S. (1965). Diamine methods for differentiating mucosubstances histochemically. J. Histochem. Cytochem. 13, 211-234.

Stein G.S., Roberts R.M., Davis J.L., Head W.J., Stein J.L., Thrall C.L., Van Veen J. and Welch D.W. (1975). Are glycoproteins and glycosaminoglycans components of the eukaryotic genome? Nature 258, 639-641.

Stevens R.L., Otsu K., Weis J.H., Tantravahi R.V., Austen K.F., Henkart P.A., Galli M.C. and Reynolds C.W. (1987). Co-sedimentation of chondroitin sulfate A glycosaminoglycans and proteoglycans with the cytolytic secretory granules of rat large granular lymphocyte (LGL) tumor cells, and identification of a mRNA in normal and transformed LGL that encodes proteoglycans. J. Immunol. 139, 863-868.

Stevens R.L., Fox C.C., Lichtenstein L.M. and Austen K.F. (1988). Identification of chondroitin sulfate E proteoglycans and heparin proteoglycans in the secretory granules of human lung mast cells. Proc. Natl. Acad. Sci. USA 85, 2284-2287.

Taper H.S. (1979). Evaluation of the validity of the histochemical lead nitrate technique for alkaline and acid deoxyribonuclease. J. Histochem. Cytochem. 27, 1483-1490.

Tassin A.-M., Celati C., Moudjou M. and Bornens M. (1998). Characterization of the human homologue of the yeast Spc98p and its association with γ-tubulin. J. Cell Biol. 141, 689-701.

Taylor S. and Folkman J. (1982). Protamine is an inhibitor of angiogenesis. Nature 297, 307-312.

Terry R.W., Bainton D.F. and Farquhar M.G. (1969). Formation and structure of specific granules in basophilic leukocytes of the guinea pig. Lab. Invest. 21, 65-76.

Tharp M.D., Seelig L.L. Jr, Tigelaar R.E. and Bergstresser P.R. (1985). Conjugated avidin binds to mast cell granules. J. Histochem. Cytochem. 33, 27-32.

Thompson H.L., Schulman E.S. and Metcalfe D.D. (1988). Identification of chondroitin sulfate E in human lung mast cells. J. Immunol. 140, 2708-2713.

Uvnäs B. and Åborg C.-H. (1976). An *in vitro*-formed protamine-heparin complex as a model for a two-compartment store for biogenic amines. Acta Physiol. Scand. 96, 512-525.

Uvnäs B. and Åborg C.-H. (1977). On the cation exchanger properties of rat mast cell granules and their storage of histamine. Acta Physiol. Scand. 100, 309-314.

Uvnäs B., Åborg C.-H. and Bergendorff A. (1970). Storage of histamine in mast cells. Evidence for an ionic binding of histamine to protein carboxyls in the granule heparin-protein complex. Acta Physiol. Scand. 78 (Suppl. 336), 1-26.

Vogel K.G. and Peterson D.W. (1981). Extracellular, surface, and intracellular proteoglycans produced by human embryo lung fibroblasts in culture (IMR-90). J. Biol. Chem. 256, 13235-13242.

Weibel E.R. and Palade G.E. (1964). New cytoplasmic components in arterial endothelia. J. Cell Biol. 23, 101-112.

Wetzel B.K., Horn R.G. and Spicer S.S. (1967). Fine structural studies on the development of heterophil, eosinophil, and basophil granulocytes in rabbits. Lab. Invest. 16, 349-382.

Wingren U. and Enerbäck L. (1983). Mucosal mast cells of the rat intestine: A re-evaluation of fixation and staining properties, with special reference to protein blocking and solubility of the granular glycosaminoglycan. Histochem. J. 15, 571-582.

Yurt R.W., Leid R.W., Austen K.F. and Silbert J.E. (1977). Native heparin from rat peritoneal mast cells. J. Biol. Chem. 252, 518-521.

Accepted September 24, 1998